学位論文

Functional analysis of Sec23 homolog Nel1 in *Saccharomyces cerevisiae*

（出芽酵母における Sec23 ホモログ Nel1 の機能解析）

平成 25 年 1 月博士(理学)申請

東京大学大学院理学系研究科

生物科学専攻

小寺 千絵

Abstract

The coat protein complex II (COPII) generates transport carriers from the endoplasmic reticulum (ER) under the control of the small GTPase Sar1. Sec23 is well known as a structural component of the COPII coat and as a GTPase-activating protein (GAP) for Sar1. Here, I showed that *Saccharomyces cerevisiae* contains a novel Sec23 homolog, Nel1, which appears not to function as a subunit of the COPII coat. Nel1 does not associate with any of the COPII components, but it exhibits strong Sar1 GAP activity. I also demonstrated that the chromosomal deletion of *NEL1* leads to a significant growth defect in the temperature-sensitive *sar1D32G* background, suggesting a possible functional link between these proteins. In contrast to Sec23, which is predominantly localized at ER exit sites on the ER membrane, a major proportion of Nel1 is localized throughout the cytosol. My findings highlight a possible role of Nel1 as a novel GAP for Sar1.

Abbreviations

COPII: coat protein complex II

EDTA: ethylenediaminetetraacetic acid

ER: endoplasmic reticulum

ERES: ER exit site

GAP: GTPase-activating protein

GDP: guanosine diphosphate

GEF: guanine nucleotide exchange factor

GFP: green fluorescent protein

GMP-PNP: guanosine-5'-[(β , γ)-imido]triphosphate

GTP: guanosine-5'-triphosphate

MBP: maltose-binding protein

Contents

Chapter I

General Introduction

1.1 Vesicular transport system in eukaryotic cells

Vesicular transport is an essential function conserved in the cells of all eukaryotic species. Newly synthesized proteins are translocated into the endoplasmic reticulum and then transported to target organelles or secreted outside the cell. Interorganelle transport is carried out by small vesicles coated with cytosolic coat protein complexes (Fig. 1). The generation of transport vesicles involves curving and budding of the donor membrane followed by membrane scission to release the vesicles (Barlowe and Miller, 2013; Brandizzi and Barlowe, 2013; D'Arcangelo et al., 2013). After the vesicles are released from the donor membrane, they move and fuse with the acceptor membrane. There are various pathways of vesicular transport, for example, endoplasmic reticulum (ER)–Golgi apparatus, intra-Golgi apparatus, endocytosis, and exocytosis (Bonifacino and Glick, 2004). The pathways are bidirectional; forward transport is called anterograde, and reverse transport is called retrograde. Recent findings support that not only small vesicles but also various other membrane structures be considered transport carriers.

Vesicular transport is responsible for the traffic of proteins and lipids in living cells. Protein secretion, elongation and migration of cells, and maintenance of organelles

also require this system. In yeast, many genes involved in vesicular transport are essential for survival. Moreover, defects in this transport system can cause several diseases in vertebrates, including human beings.

To investigate molecular mechanisms of vesicular transport, yeast genetics has been a powerful technique. When research on the secretory system commenced, numerous mutants with defective protein secretion were isolated by an elegant screening system using *Saccharomyces cerevisiae* (Novick et al., 1980). *In vitro* systems in yeast and mammals have also revealed deep insights in this area (Balch et al., 1984; Matsuoka et al., 1998), and the development of imaging systems has been key in demonstrating membrane dynamics in living cells (Losev et al., 2006; Matsuura-Tokita et al., 2006).

1.2 Early secretory pathway

The anterograde transport from the ER to the Golgi complex is the gateway of vesicular transport. Transport vesicles from the ER, 50–60 nm in diameter, are called coat protein complex II (COPII)-coated vesicles. The basic mechanism of COPII vesicle formation is well characterized in yeast (Fig. 2). The small GTPase Sar1 plays a key role

in this process (Barlowe et al., 1993; Barlowe et al., 1994; Nakano and Muramatsu, 1989). GDP-bound Sar1 in the cytosol is converted to a GTP-bound form by an ER-localized guanine nucleotide exchange factor (GEF) Sec12 (Barlowe and Schekman, 1993; Nakano et al., 1988). GTP-bound Sar1 exposes its N-terminal amphipathic helix and inserts it into the ER membrane. Sar1-GTP recruits inner coat protein complex Sec23/24. Sec23 is a GTPase activating protein (GAP) for Sar1, and Sec24 presents a key portion to capture cargo proteins (Bi et al., 2002; Miller et al., 2003; Mossessova et al., 2003). This Sar1-Sec23/24-cargo complex is called the pre-budding complex. Subsequently, the outer coat subunit Sec13/31 bridges pre-budding complexes (Bi et al., 2007; Tabata et al., 2009). By this process, membrane curvature is induced, and finally, vesicle scission and release occur (Fig. 2).

1.3 COPII components and players involved in COPII vesicle formation

1.3.1 Sar1

Sar1 was identified as a multicopy suppressor of the *sec12* temperature-sensitive mutant (Nakano and Muramatsu, 1989). It has homology to Ras-like GTPase. The GTP-

GDP cycle of Sar1 has been known to have multiple roles in regulating COPII vesicle formation. At an early stage of vesicle formation, GTP-bound Sar1 recruits Sec23/24 to the ER membrane. During pre-budding complex formation, cargo selection and concentration occur through multiple rounds of Sar1 GTP hydrolysis (Sato and Nakano, 2005; Tabata et al., 2009). The insertion of the Sar1-GTP amphipathic helix can impart membrane curvature (Lee et al., 2005). In addition to the insertion of the helix, Sar1 concentration is also important for generating membrane curvature. (Settles et al., 2010). One isoform of Sar1 exists in *S. cerevisiae*, but in many higher eukaryotes, two homologs have been reported. In mammalian cells, Sar1B is responsible for transporting large cargos by making huge COPII carriers. Moreover, different Sar1 isoforms are associated with distinct diseases in humans (Miller and Schekman, 2013).

1.3.2 Sec23/24 and Sec13/31

Sec23/24 is a heterodimeric complex, which forms the inner coat of COPII vesicles. Sec23/24 binds to the membrane via Sec23-Sar1-GTP interaction (Bi et al., 2002). In addition, the electrical interaction between Sec23/24 and phospholipids in the

membrane also serves to secure binding (Matsuoka et al., 1998). The C-terminal Arg residue of Sec23 is directly involved in accelerating Sar1 GTPase activity (Bi et al., 2002). Sec24 and its homologs in yeast, Lst1 and Iss1, form stable complexes with Sec23, and they function as cargo selection players. Sec24 and its homologs capture cytosolic signals of cargos directly or indirectly (Kurihara et al., 2000; Miller et al., 2003; Shimoni et al., 2000). Some adaptor proteins have also been reported (Belden and Barlowe, 2001; Bue and Barlowe, 2009).

Sec13/31 is a heterotetrameric complex which forms the outer coat of COPII vesicles (Bi et al., 2007). Sar1, Sec23/24 and Sec13/31 are the minimum components required for COPII vesicle formation *in vitro* (Matsuoka et al., 1998). Sec13/31 stimulates Sec23-accelerated Sar1 GTP hydrolysis by about tenfold and polymerizes pre-budding complexes (Antonny et al., 2001; Bi et al., 2007).

1.3.3 Sec12 and Sed4

Sec12 is the initiation factor of the COPII vesicle formation, converting Sar1 from its GDP-form to GTP-form by its strong GEF activity. It is a type II membrane protein

located in the ER, and a deletion mutant of Sec12 is lethal (Barlowe and Schekman, 1993; Nakano et al., 1988). The Sec12 C-terminal region of *S. cerevisiae* is shorter than that of *Pichia pastoris* or higher eukaryotes (Payne et al., 2000).

Sed4 is homolog of Sec12 unique to *S. cerevisiae*. The Sed4 N-terminal catalytic region has 45% identity to that of Sec12, and it has a long C-terminal region. Unlike Sec12, the Sed4 deletion mutant is not lethal (Gimeno et al., 1995; Hardwick et al., 1992). Despite its similarity to Sec12, Sed4 has no GEF activity for Sar1 (Kodera et al., 2011; Saito-Nakano and Nakano, 2000). Interestingly, Sed4 stimulates Sar1 GTPase activity when Sar1 does not bind to the cargo molecules. Therefore, Sed4 seems to contribute to cargo concentration into the COPII vesicle by regulating Sar1-GTP hydrolysis (Kodera et al., 2011).

1.3.4 Sec16

Sec16 is a large (250-kDa) peripheral membrane protein, and it is not required for COPII vesicle formation in the reconstitution system. However, it is needed for ER–Golgi transport in living cells. Moreover, Sec16 is essential for yeast survival (Espenshade et

al., 1995; Watson et al., 2006). Sec16 binds to all COPII components (Sar1, Sec23/24, Sec13/31), Sec12 (not in *S. cerevisiae*), and Sed4. Sec16 has been thought to be a scaffold protein for COPII coat assembly (Gimeno et al., 1995, 1996; Montegna et al., 2012; Whittle and Schwartz, 2010). In addition, recent studies have shown that Sec16 regulates Sar1 GTP hydrolysis. Sec16 inhibits Sec31-stimulated Sec23 GAP activity and appears to stabilize coat proteins until COPII vesicles are fully generated (Kung et al., 2012; Yorimitsu and Sato, 2012).

1.4 ER-exit site

The COPII vesicle is generated at a specialized site called the ER-exit site (ERES) (Barlowe and Miller, 2013; Brandizzi and Barlowe, 2013; D'Arcangelo et al., 2013). The ERES is a dot-like structure on the ER membrane, and there are numerous ERESs in yeast cells. Coat proteins and Sec16 concentrate at this site (Okamoto et al., 2012; Shindiapina and Barlowe, 2010; Yorimitsu and Sato, 2012). Interestingly, Sec12 is concentrated at ERES in *P. pastoris* but not in *S. cerevisiae* (Montegna et al., 2012; Okamoto et al., 2012; Soderholm et al., 2004). Sec16 has been considered to act as a scaffold protein at the

initial stages of ERES formation. Sec16 contributes to the recruitment of the COPII coat proteins to liposomes (Supek et al., 2002). ERES localization patterns of COPII coat proteins are altered in temperature-sensitive mutant *sec12-4* at non-permissive temperatures, but Sec16 is not affected (Okamoto et al., 2012). Sec16 also exhibits self-oligomerization ability on the liposome (Yorimitsu and Sato, 2012).

In plant cells, cis-Golgi is known to be localized near the ERES, and recently, yeast cis-Golgi was shown to be localized opposite to the ERES (Brandizzi and Barlowe, 2013).

1.5 Sec23 homologs

As mentioned above, the Sar1-GTPase cycle regulates many steps of COPII vesicle generation, and multiple players modulate Sar1-GTP hydrolysis (D'Arcangelo et al., 2013). A crucial one is Sec23, a GAP for Sar1. Many species have two or more Sec23 homologs (Miller and Schekman, 2013; West et al., 2011). In humans, cranio-lenticulo-sutural dysplasia, a disease associated with a defect in collagen secretion, is caused by a SEC23A mutation (Boyadjiev et al., 2006). A SEC23B mutant is associated with

congenital dyserythropoietic anemia type II (Schwarz et al., 2009). In yeast, *P. pastoris* has been reported to have a Sec23 homolog Shl23, which is localized at the ERES and is associated with Sec24 homolog Lst1 (Esaki et al., 2006). To our knowledge, previously reported Sec23 homologs are all concentrated at the ERES and are considered to be involved in COPII carrier formation (Rossanese et al., 1999; Shindiapina and Barlowe, 2010). However, the functional diversity of these isoforms has not been fully characterized.

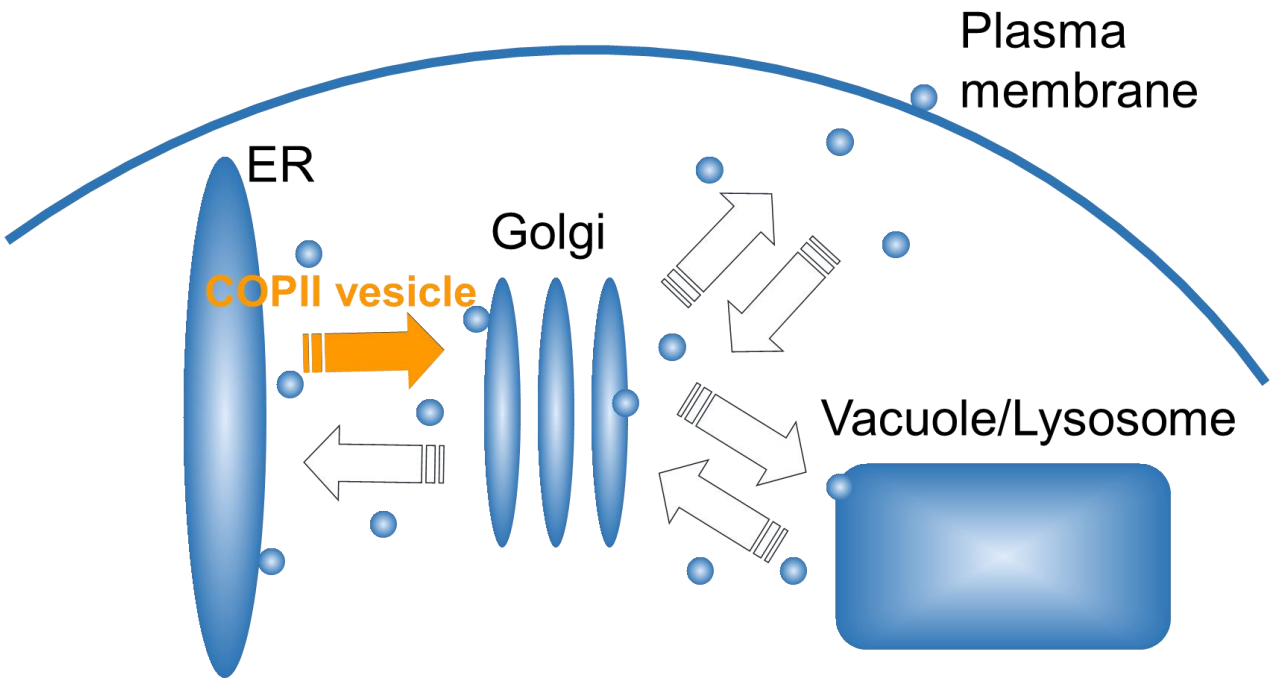

Figure 1. Schematic model of vesicular transport.

Small vesicles are responsible for the inter organelle transport. COPII vesicles are considered to be transported from the ER to the Golgi.

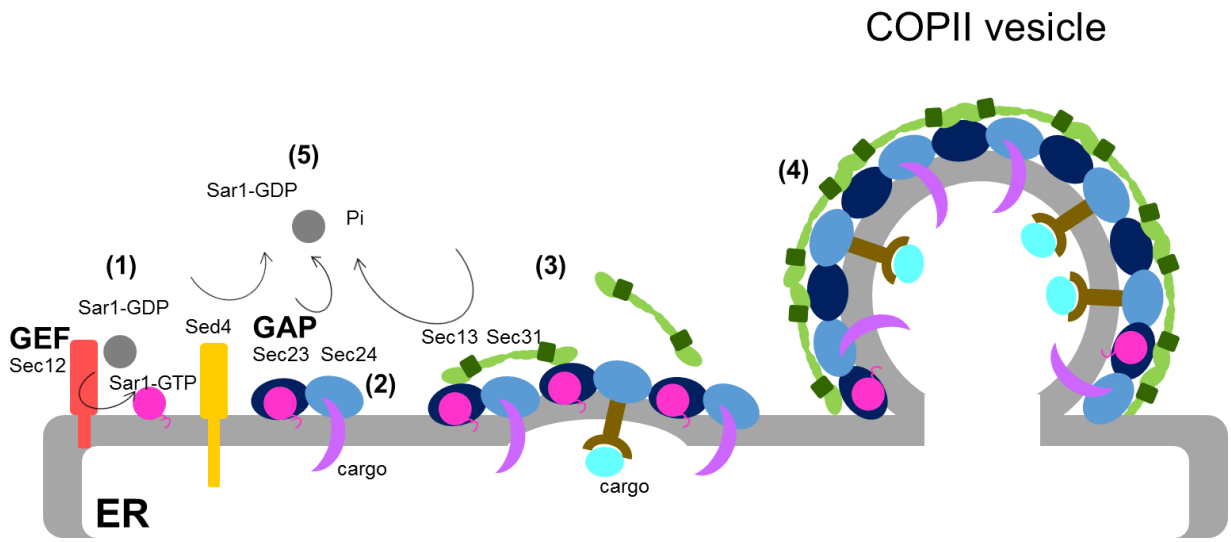

Figure 2. Schematic model for molecular mechanism of the COPII vesicle formation.

Sar1-GDP is transformed to Sar1-GTP by ER-located GEF, Sec12 (1). Sar1-GTP binds to ER membrane and recruits COPII inner coat protein Sec23/24 (2). Sar1-Sec23/24 complex (pre-budding complex) is polymerized by outer coat Sec13/31 (3). Coat assembly causes membrane curvature (4). Sar1 GTPase cycle is regulated by several proteins through the COPII vesicle formation (5).

Chapter II

Introduction

In eukaryotic cells, newly synthesized membrane and soluble proteins in the endoplasmic reticulum (ER) destined for export to the Golgi or beyond are concentrated at specialized ER exit sites (ERES), where they are packaged into transport carriers generated by COPII coat proteins (Barlowe and Miller, 2013; Brandizzi and Barlowe, 2013; D'Arcangelo et al., 2013). The COPII coat consists of an inner layer of the Sec23/24 heterodimeric complex surrounded by an outer layer of the Sec13/31 heterotetramer complex, and these components are sequentially assembled onto the ER membrane through the action of the small GTPase Sar1 (Barlowe et al., 1993; Barlowe et al., 1994; Nakano and Muramatsu, 1989). In brief, the assembly of the COPII coat is triggered by a GDP-GTP exchange on Sar1 that is catalyzed by the ER-resident guanine nucleotide exchange factor Sec12 (Barlowe and Schekman, 1993; Nakano et al., 1988). The activated Sar1-GTP binds to the ER membranes and recruits the Sec23/24 complex by binding to the Sec23 portion, and the Sec24 subunit captures the cargo protein to form a pre-budding complex (Bi et al., 2002; Miller et al., 2003; Mossessova et al., 2003). Subsequently, the outer layer of the Sec13/31 complex is recruited onto Sec23/24, which polymerizes adjacent pre-budding complexes to drive membrane deformation (Bi et al.,

2007; Tabata et al., 2009). The Sec23 subunit is the GTPase-activating protein (GAP) for Sar1, and repeated cycles of Sec12-dependent GTP loading to Sar1 and Sec23-mediated hydrolysis facilitate proper and efficient cargo sorting into COPII vesicles (Antonny et al., 2001; Futai et al., 2004; Sato and Nakano, 2005; Yoshihisa et al., 1993). Thus, Sec23 acts both as a component of the COPII coat structure and as the GAP for the small GTPase Sar1, as well as regulating COPII assembly. Recent findings have suggested that GTPase inhibitory activity mediated by the peripheral membrane protein Sec16 also modulates the assembly of the COPII coat at ERES (Kung et al., 2012; Yorimitsu and Sato, 2012).

In humans and many other species, gene duplication events generate multiple homologs for most of these COPII components (Miller and Schekman, 2013). However, it is not clear whether these COPII homologs are functionally redundant, or whether their multiplication represents an adaptation to either the increased complexity of cargo proteins or to the tissue-specific requirements. Although most eukaryotes carry two homologs of Sec23 (Paccaud et al., 1996), no Sec23 homologs have been described in *Saccharomyces cerevisiae* to date. In the present study, I show that *S. cerevisiae* contains a novel Sec23 homolog that I designated Nel1 (Non-ERES Localized Sec23 homolog 1),

which appears to have a function distinct from that of Sec23. I found that purified Nel1 activates the GTPase activity of Sar1 but does not associate with any of the COPII coat components. Nel1 is predominantly localized throughout the cytosol, and the chromosomal disruption of *NEL1* affects the growth phenotype of the temperature-sensitive *sar1* mutant. My findings provide a possible functional link between Sar1 and its novel GAP, Nel1.

Chapter III

Experimental Procedures

3.1 Strains and media

The strains used in this study are listed in Table 1. Gene deletions were performed by a PCR-based procedure using the plasmid pUG73 as a template (Gueldener et al., 2002). CKY1, CKY2, and CKY3 were generated from ANY21 (Nakano et al., 1988), TOY221, and TOY223 (Saito et al., 1999), respectively. Unless otherwise noted, the cultures were grown at 30°C in YPD medium (1% Bacto-yeast extract, 2% polypeptone, and 2% dextrose), MVD medium (2% dextrose and 0.67% yeast nitrogen base without amino acids), MCD medium (0.67% yeast nitrogen base without amino acids, 0.5% casamino acids, and 2% dextrose), or MCGS medium (0.67% yeast nitrogen base without amino acids, 0.5% casamino acids, 5% galactose, and 0.2% sucrose) supplemented appropriately.

Table 1. Yeast strains used in this study

Strain	Genotype	Reference
ANY21	*MAT*a *ura3-52 leu2-3,112 trp1-289 his3 his4 suc gal2*	(Nakano et al., 1988)
CKY1	*MAT*a *nel1Δ::LEU2 ura3-52 leu2-3,112 trp1-289 his3 his4 suc gal2*	This study
CKY2	*MATa nel1Δ::LEU2 sar1Δ::HIS3 pep4::ADE2 ura3 leu2 trp1 his3 ade2 lys2* /pMYY3-l (YCp [SAR1 *TRP1])*	This study
CKY3	*MATα nel1Δ::LEU2 sar1Δ::HIS3 pep4::ADE2 ura3 leu2 trp1 his3 ade2 lys2* / pMYY3-7 (YCp[*sar1D32G TRP1*])	This study
MBY8-20C	*MAT*a *sec23-1 ura3-52 leu2-3,112 trp1-289 his3 his4*	Bernstein and Schekman
PJ69-4A	*MATa* t*rp1-901 leu2-3,112 ura3-52 his3-200 gal4Δ gal80Δ GAL2-ADE2 LYS2*::*GAL1-HIS3 met2*::*GAL7-lacZ*	(James et al., 1996)
TOY221	*MATa sar1Δ::HIS3 pep4::ADE2 ura3 leu2 trp1 his3 ade2 lys2* / pMYY3-l (YCp [SAR1 *TRP1])*	(Saito et al., 1999)
TOY223	*MATα sar1Δ::HIS3 pep4::ADE2 ura3 leu2 trp1 his3 ade2 lys2* / pMYY3-7 (YCp[*sar1D32G TRP1*])	(Saito et al., 1999)
YPH500	*MATα ura3-52 lys2-801_amber ade2-101_ochre trp1-Δ63 his3-Δ200 leu2-Δ1*	(Sikorski and Hieter, 1989)

3.2 Plasmid construction

The coding sequences of the *NEL1* gene or the *SEC23* gene, together with its upstream and downstream flanking regions, were amplified by PCR using the *S. cerevisiae* genomic DNA and inserted into the *Not*I and *Bam*HI (*NEL1*) or the *Bam*HI and *Sal*I (*SEC23*) sites of pRS316 (*CEN, URA3*), yielding pNEL1/316 and pSEC23/316, respectively. A fragment including the *TDH3* promoter and *CMK1* terminator was inserted into the *Bam*HI and *Sal*I sites of pRS316, pYO326 (*2μ, URA3*), pYO324 (*2μ, TRP1*), and pRS314 (*CEN, TRP*), yielding pCKY4, pCKY5, pCKY6, and pCKY8, respectively. The coding sequences of the *NEL1* and *SEC23* genes were amplified by PCR from yeast genomic DNA and inserted into the *Bgl*II site (located between *TDH3* promoter and *CMK1* terminator) of pCKY5, yielding pNEL1/CKY5 and pSEC23/CKY5, respectively. To generate plasmids for yeast two-hybrid analysis, *NEL1* was cloned into the *Bgl*II sites of pGAD-C1 and pGBDU-C1 (James et al., 1996). *SEC24*, which was digested with *Sma*I and *Xho*I, was cloned into the *Sma*I and *Sal*I sites of pGAD-C1 and pGBDU-C1. *SEC23*, *LST1*, and *ISS1* were cloned into the *Bam*HI and *Sal*I, *Eco*RI and *Bam*HI, and *Bam*HI and *Pst*I sites, respectively, of pGAD-C1. For Nel1-MBP purification,

the coding sequence of *NEL1* together with a myc-tag at the N-terminus and a *Sph*I site just before the stop codon was amplified by PCR from yeast genomic DNA and inserted into the *Bgl*II site of pCKY6, and a fragment encoding MBP, amplified by PCR from pMAL-c2x (New England BioLabs), was inserted into the *Sph*I site, yielding pNEL1-MBP/CKY6. For Nel1-R592A-MBP purification, the R592A mutation was introduced into pNEL1-MBP/CKY6 by primer-directed mutagenesis, yielding pNEL1-R592A-MBP/CKY6. For pull-down assay, plasmids expressing Sec24-HA, Lst1-HA, or Iss1-HA under the *GAL* promoter were obtained from Yeast ORF collection (Open Biosystems). A fragment encoding MBP together with a myc-tag at the N-terminus was amplified by PCR from pMAL-c2x and inserted into the *Bgl*II site of pCKY8, yielding pMBP/CKY8. The coding sequence of *SEC23* together with a myc-tag at the N-terminus and a *Xma*I site just before the stop codon was amplified by PCR from yeast genomic DNA and inserted into the *Sac*I and *Xho*I sites of pYES3/CT (Life technologies), and a fragment encoding MBP, amplified by PCR from pMAL-c2x, was inserted into the *Xma*I site, yielding pSEC23-MBP/YES3. To obtain the plasmid pNEL1-13Myc/316, I first generated a yeast strain CKY4 by a PCR-based procedure using pFA6a-13Myc-TRP1

(Longtine et al., 1998), which chromosomally expresses C-terminally 13myc-tagged Nel1. The coding sequence of the Nel1-13myc, together with its upstream and downstream flanking regions, was amplified by PCR from the genome of the CKY4 strain and inserted into the *Not*I and *Bam*HI sites of pRS316, yielding pNEL1-13Myc/316. The fragment encoding EGFP was inserted into the *Bgl*II and *Hind*III sites of pCKY4, yielding pCKY7. The coding region of *NEL1*, amplified by PCR from yeast genomic DNA, was inserted into the *Bgl*II site of pCKY7, yielding pNEL1/CKY7. The coding sequences of the *NEL1* and *HTB1* genes, together with their upstream and downstream flanking regions, were amplified by PCR from yeast genomic DNA and inserted into the *Not*I and *Bam*HI (*NEL1*) and *Not*I and *Xho*I (*HTB1*) sites of pRS314 (*CEN, TRP1*), yielding pNEL1/314 and pHTB1/314, respectively. For the fluorescent protein fusions, *Sph*I (*NEL1*) and *Bam*HI (*HTB1*) sites were created just before the stop codon of each gene. Then, fragments encoding mCherry and AcGFP (Clontech, Mountain View, CA) were inserted into the *Sph*I (Nel1-mCherry) and *Bam*HI (Htb1-GFP) sites, yielding pNEL1-mCherry/314 and pHTB1-GFP/314, respectively. A fragment encoding NEL1-mCherry, amplified by PCR from pNEL1-mCherry/314, was then inserted into the *Bgl*II site of

pCKY4, yielding pNEL1-mCherry/CKY4.

3.3 Protein preparation

Sar1, Sec23/24, and Sec13/31 were purified as described previously (Barlowe et al., 1994; Matsuoka and Schekman, 2000). In brief, Sar1-GST was expressed in *E. coli*, bound to glutathione sepharose, and eluted by cleaving the GST moiety with thrombin (Fig. 3). A His6-tagged version of Sec24 was co-overexpressed with Sec23 in *S. cerevisiae* and purified as a complex by Ni-NTA affinity chromatography followed by diethylaminoethyl chromatography (Fig. 4). A His6-tagged version of Sec31 was co-overexpressed with Sec13 in *S. cerevisiae* and purified as a complex by Ni-NTA affinity chromatography and subjected to Q Sepharose chromatography (Fig. 5). Nel1-MBP and Nel1-R592A-MBP were purified from yeast YPH500 cells carrying the pNEL1-MBP/CKY6 or pNEL1-R592A-MBP/CKY6 plasmids, respectively. The cells were grown to late-log phase at 30°C. The cells from 12 L of cultures were washed with distilled water and then resuspended in suspension buffer (50 mM HEPES-KOH, pH 7.4, 500 mM KoAc, 5 mM EDTA, 10% glycerol) containing a 3× protease inhibitor cocktail

(PIC; Roche). The cell suspension was frozen as drops by pouring it into liquid nitrogen and then stored at −80°C. The frozen cells were subsequently blended and thawed on ice. From the supernatant obtained from a 20 min centrifugation at 9,500 rpm with a JA-14 rotor (Beckman Coulter) at 4°C, the protein extract was recovered by ultracentrifugation at 42,000 rpm for 1 h at 4°C in a Hitachi P45AT rotor. The supernatant was incubated with amylose resin (New England BioLabs) for 1.5 h at 4°C. The resin was washed with wash buffer 1 (20 mM HEPES-KOH, pH 7.4, 500 mM KoAc, 5 mM EDTA, 10% glycerol) and then with wash buffer 2 (20 mM HEPES-KOH, pH 7.4, 500 mM KoAc, 1 mM EDTA, 10% glycerol). Nel1-MBP and Nel1-R592A-MBP were eluted with elution buffer (20 mM HEPES-KOH, pH 7.4, 500 mM KoAc, 50 mM maltose, 10% glycerol).

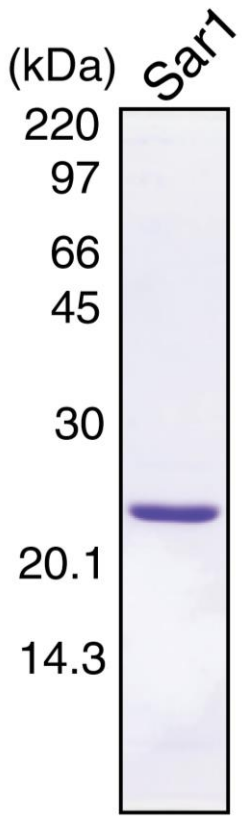

Figure 3. Sar1 was purified from *E. coli* cells.

Protein from JM109 cells expressing GST-Sar1 was purified by glutathione sepharose, by cleaving GST moiety with thrombin, and separated by SDS-PAGE followed by staining with Coomassie brilliant blue.

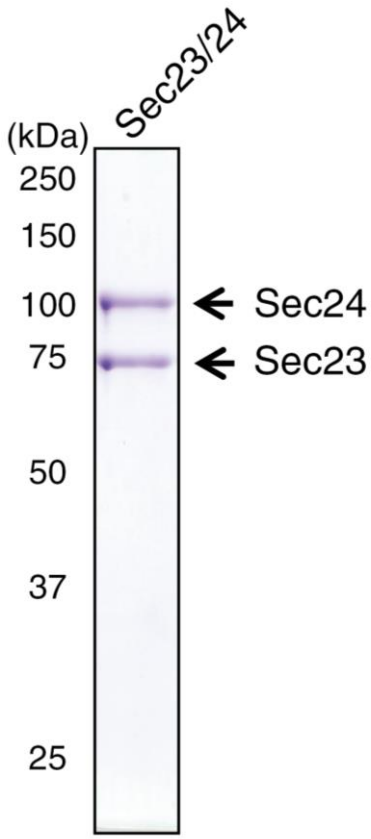

Figure 4. Sec23/24 was purified from *S. cerevisiae* cells.

A His6-tagged version of Sec24 co-overexpressed with Sec23 in *S. cerevisiae* was purified as a complex by Ni-NTA affinity chromatography followed by diethylaminoethyl chromatography, and separated by SDS-PAGE followed by staining with Coomassie brilliant blue.

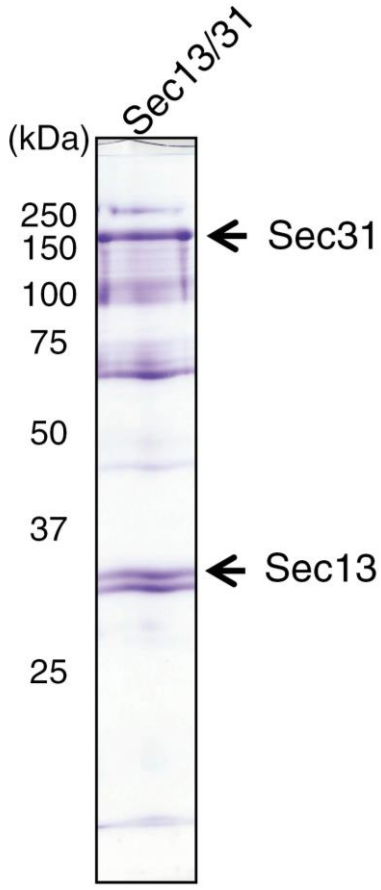

Figure 5. Sec13/31 was purified from *S. cerevisiae* cells.

A His6-tagged version of Sec31 co-overexpressed with Sec13 in *S. cerevisiae* was purified as a complex by Ni-NTA affinity chromatography, subjected to Q Sepharose chromatography and separated by SDS-PAGE followed by staining with Coomassie brilliant blue.

3.4 Pull-down assay

YPH500 cells carrying the appropriate plasmids were pregrown to mid-log phase at 30°C in MCD medium and then transferred to MCGS medium. After 2.5 h incubation, 20 OD units of cells (per sample) were harvested and resuspended in suspension buffer (20 mM HEPES-KOH, pH 7.4, 500 mM KoAc, 5 mM EDTA, 10% glycerol). The cells were disrupted by vortex mixing with glass beads at 4°C, and protein extracts were incubated with amylose resin for 1 h at 4°C. The resins were washed with the suspension buffer and samples were eluted by elution buffer (20 mM HEPES-KOH, pH 7.4, 500 mM KoAc, 50 mM maltose, 10% glycerol). The samples were then analyzed by SDS-PAGE and immunoblotting.

3.5 Tryptophan fluorescence measurements and liposome-binding assay

Tryptophan fluorescence measurements and liposome-binding assays were carried out as described previously (Antonny et al., 2001; Sato and Nakano, 2005). For tryptophan fluorescence measurements, Sar1, liposomes, and GTP were mixed with reaction buffer (20 mM HEPES-KOH, pH 6.8, 160 mM KoAc, 1 mM $MgCl_2$) (total

volume, 200 μl), and incubated in a quartz cuvette for 500 sec to convert Sar1-GDP to Sar1-GTP. Then, Sec23/24 or Nel1 was injected with Hitachi 50 μl syringe to start reaction. Tryptophan fluorescence (excitation, 298 nm; emission, 340 nm) was measured in the cuvette with a Hitachi fluorescence spectrophotometer (F-2500) equipped with a thermostatically controlled cell holder and magnetic stirrer. All experiments were performed at 25°C. For liposome-binding assay, proteins, liposomes, and GMP-PNP, or GDP in reaction buffer (total volume 300 μl) were incubated at 30°C for 15min, and then placed on ice to stop reaction. The concentration of sucrose in each reaction was adjusted to 1 M by the addition of 200 μl reaction buffer containing 2.5 M sucrose. 400 μl of the each mixture were transferred to centrifuge tubes (HITACHI S308892A) and overlaid with 400 μl of reaction buffer containing 0.75 M sucrose and 100 μl of reaction buffer. The resulting step gradient samples were centrifuged at 55,000 rpm in a HITACHI S55A2 rotor for 2 h at 4 °C. Samples (200 μl) were collected from the top of each tube. The recovery of the lipid was determined by recording the fluorescence of liposome with a LAS3000 image analyzer. After normalization for lipid recovery, proteins were precipitated by trichloroacetate, separated by SDS–PAGE, stained by SYPRO Orange

(Life Technologies), and detected with a LAS3000 image analyzer. All experiments were performed with synthetic major–minor mix liposomes (Matsuoka et al., 1998).

3.6 Fluorescence microscopy

Yeast cells expressing fluorescent proteins were grown to mid-log phase at 23°C. Fluorescence microscopy observations were carried out using an Olympus IX71 microscope (Olympus) equipped with a CSU10 spinning-disk confocal scanner (Yokogawa Electric Corporation) and an electron-multiplying charge-coupled device camera (iXon, DV897; Andor Technology). The acquired images were analyzed using Andor iQ (Andor Technology). In this setting, a 473 nm solid-state laser (J050BS; Showa Optronics) was used to excite AcGFP, EGFP, and mCherry at 561 nm (Jive; Cobolt).

3.7 Subcellular fractionation

Subcellular fractionation was performed as described previously (Vida et al., 1990). In brief, CKY1 cells carrying pNEL1-13Myc/316 were grown to mid-log phase and 500 OD units of cells (per sample) were converted to spheroplasts by treatment with

Zymolyase. The spheroplasts were resuspended in 2× lysis buffer (40 mM HEPES-KOH, pH 7.4, 400 mM sorbitol, 100 mM KoAc, 4 mM EDTA, supplemented with PIC and 1 mM DTT) and then centrifuged at 3,000 rpm for 10 min in a Beckman JA-14 rotor. The spheroplast pellets were resuspended in lysis buffer (20 mM HEPES-KOH, pH 7.4, 200 mM sorbitol, 50 mM KoAc, 2 mM EDTA, supplemented with PIC and 1 mM DTT) and then subjected to seven strokes in a Dounce homogenizer. The lysates were centrifuged at 300 × *g* for 5 min to remove unbroken materials, yielding the total fractions (S3). The total fractions were centrifuged at 13,000 × *g* for 15 min to generate the S13 supernatants and P13 pellets. The P13 pellets were washed four times with lysis buffer. The samples (about 50 OD units of cells each) were then analyzed by SDS-PAGE and immunoblotting. Signals were analyzed by Lighting Ultra Extreme Sensitivity Chemiluminescence Substrate (Perkin Elmer) and LAS300 image analyzer. Myc antibody 9E-10 (BAbCO), Pgk1 antibody #459250 (Invitrogen), Nop1 antibody MCA-28F (EnCor), Dpm1 antibody A6429 (Invitrogen), and Sec23 antibody (Hicke and Schekman, 1989) were used.

.

Chapter IV

Results

4.1 NEL1, a gene encoding a Sec23-like protein

A search of the yeast *Saccharomyces cerevisiae* genome revealed an uncharacterized open reading frame, YHR035W, which encodes a 630-amino acid nonessential protein with sequence similarity to members of the Sec23 family and which I designated Nel1. Alignment analysis using ClustalX revealed that Nel1 has strong similarity to Sec23, with 21% identity and 37% similarity. Nel1 contains a putative catalytic arginine residue (R592) necessary for the GAP activity on Sar1 (Fig. 6) (Bi et al., 2002).

Given the sequence similarity of Nel1 to Sec23, I first examined whether Nel1 could complement the temperature sensitivity of a *sec23-1* mutant (Novick et al., 1980). Since *sec23-1* cells already have a chromosomal copy of *NEL1*, endogenous expression of Nel1 is clearly not sufficient to rescue the temperature-sensitive phenotype of the *sec23-1* strain. However, even high-copy expression of Nel1 under the control of a strong constitutive *TDH3* promoter could not suppress the temperature-sensitive growth defect of the *sec23-1* mutant (Fig. 7). In addition, overexpression of Nel1 was not found to have obvious effects on growth of the other early *sec* mutants tested (*sar1D32G, sar1E112K,*

sar1N132I, *sec12-4*, *sec13-1*, or *sec16-2*). A previous study has shown that overexpression of Sec23 leads to growth inhibition in wild-type cells, presumably by disturbing the GDP/GTP cycling of Sar1 through the excess GAP activity of Sec23 (Kurihara et al., 2000). However, overexpression of Nel1 did not cause any apparent growth defect in wild-type cells (Fig. 8). The combined results suggest that Nel1 activity is not functionally redundant with Sec23, thus suggesting a specialized role(s) for this protein *in vivo*.

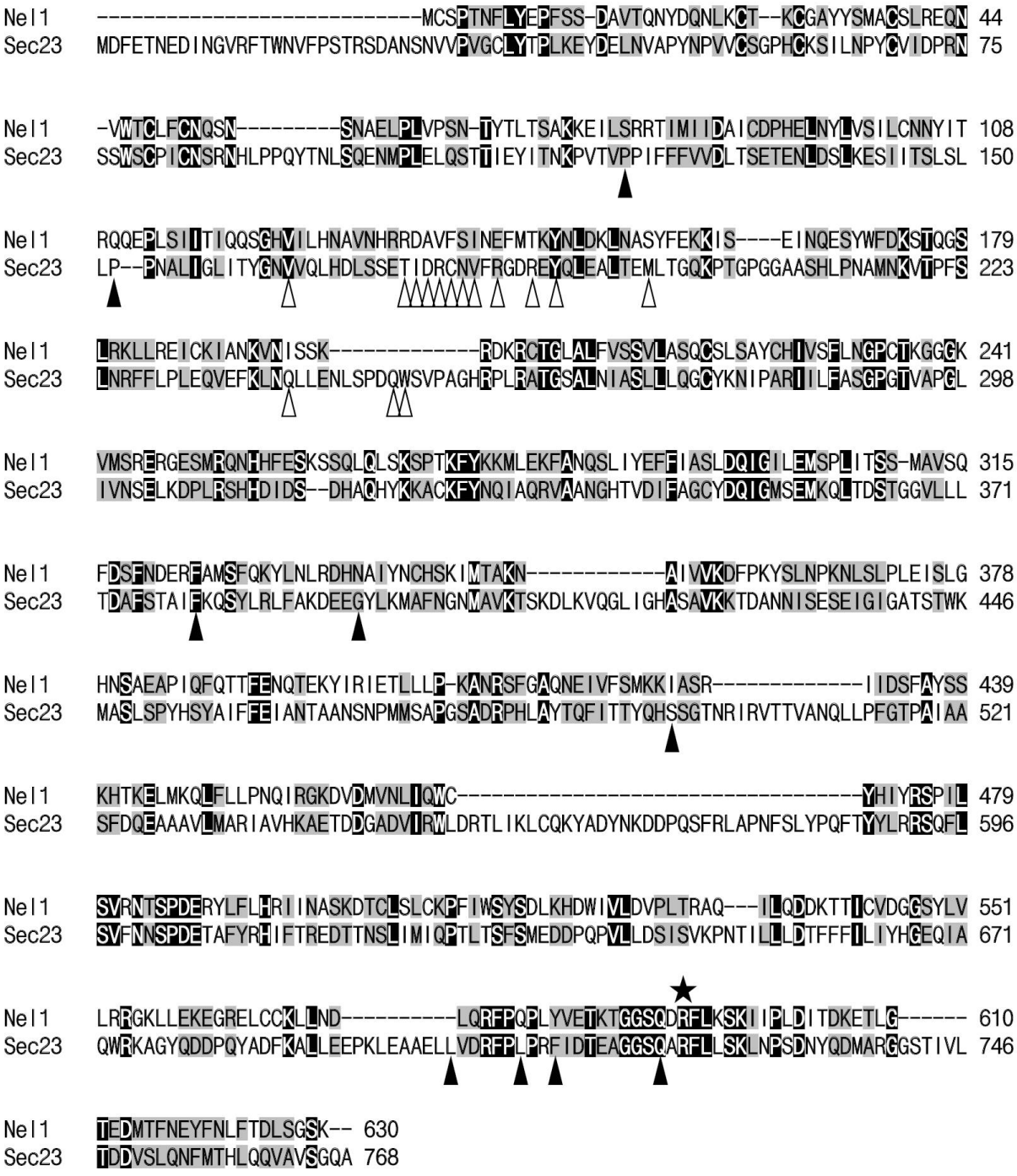
Nel1 ----------MCSPTNFLYEPFSS-DAVTQNYDQNLKCT--KCGAYYSMACSLREQN 44
Sec23 MDFETNEDINGVRFTWNVFPSTRSDANSNVVPVGCLYTPLKEYDELNVAPYNPVVCSGPHCKSILNPYCVIDPRN 75
Nel1 -VWTCLFCNQSN---------SNAELPLVPSN-TYTLTSAKKEILSRRTIMIIDAICDPHELNYLVSILCNNYIT 108
Sec23 SSWSCPICNSRNHLPPQYTNLSQENMPLELQSTTIEYITNKPVTVPPIFFFVVDLTSETENLDSLKESIITSLSL 150
Nel1 RQQEPLSIITIQQSGHVILHNAVNHRRDAVFSINEFMTKYNLDKLNASYFEKKIS----EINQESYWFDKSTQGS 179
Sec23 LP--PNALIGLITYGNVVQLHDLSSETIDRCNVFRGDREYQLEALTEMLTGQKPTGPGGAASHLPNAMNKVTPFS 223
Nel1 LRKLLREICKIANKVNISSK----------RDKRCTGLALFVSSVLASQCSLSAYCHIVSFLNGPCTKGGGK 241
Sec23 LNRFFLPLEQVEFKLNQLLENLSPDQWSVPAGHRPLRATGSALNIASLLLQGCYKNIPARIILFASGPGTVAPGL 298
Nel1 VMSRERGESMRQNHHFESKSSQLQLSKSPTKFYKKMLEKFANQSLIYEFFIASLDQIGILEMSPLITSS-MAVSQ 315
Sec23 IVNSELKDPLRSHFDIDS--DHAQHYKKACKFYNQIAQRVAANGHTVDIFAGCYDQIGMSEMKQLTDSTGGVLLL 371
Nel1 FDSFNDERFAMSFQKYLNLRDHNAIYNCHSKIMTAKN----------AIVVKDFPKYSLNPKNLSLPLEISLG 378
Sec23 TDAFSTAIFKQSYLRLFAKDEEGYLKMAFNGNMAVKTSKDLKVQGLIGHASAVKKTDANNISESEIGIGATSTWK 446
Nel1 HNSAEAPIQFQTTFENQTEKYIRIETLLLP-KANRSFGAQNEIVFSMKKIASR----------IIDSFAYSS 439
Sec23 MASLSPYHSYAIFFEIANTAANSNPMMSAPGSADRPHLAYTQFITTYQHSSGTNRIRVTTVANQLLPFGTPAIAA 521
Nel1 KHTKELMKQLFLLPNQIRGKDVDMVNLIQWC----------YHIYRSPIL 479
Sec23 SFDQEAAAVLMARIAVHKAETDDGADVIRWLDRTLIKLCQKYADYNKDDPQSFRLAPNFSLYPQFTYYLRRSQFL 596
Nel1 SVRNTSPDERYLFLHRIINASKDTCLSLCKPFIWSYSDLKHDWIVLDVPLTRAQ---ILQDDKTTICVDGGSYLV 551
Sec23 SVFNNSPDETAFYRHIFTREDTTNSLIMIQPTLTSFSMEDDPQPVLLDSISVKPNTILLLDTFFFILIYHGEQIA 671
Nel1 LRRGKLLEKEGRELCCKLLND----------LQRFPQPLYVETKTGGSQDRFLKSKIIPLDITDKETLG------ 610
Sec23 QWRKAGYQDDPQYADFKALLEEPKLEAAELLVDRFPLPRFIDTEAGGSQARFLLSKLNPSDNYQDMARGGSTIVL 746
Nel1 TEDMTFNEYFNLFTDLSGSK-- 630
Sec23 TDDVSLQNFMTHLQQVAVSGQA 768

Figure 6. Pairwise sequence alignment of Sec23 and its closest homolog, Yhr035w.

The optimal alignment was obtained by using the ClustalX program. Highlighted residues (white letters on black) indicate amino acids that are identical to those of Sec23, and grey residues indicate conservation. The star indicates the catalytic arginine residue necessary for Sec23 GAP activity. Arrowheads indicate residues making intersubunit interactions between Sec23/Sec24 (white) and Sec23/Sec31 (black).

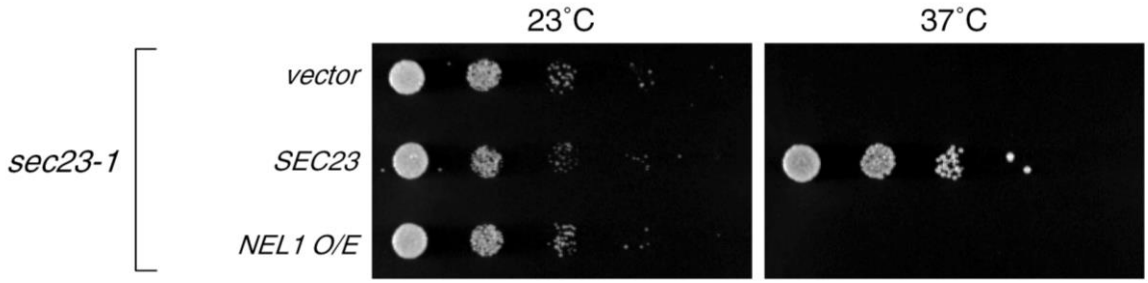

Figure 7. Nel1 overexpression cannot compensate for the loss of Sec23 function.

The *sec23-1* cells were transformed with pCKY5 (*2μ* vector), pNEL1/CKY5 (*2μ NEL1*), or pSEC23/316 (*CEN SEC23*). The *SEC23* gene was expressed from its own promoter on a single-copy plasmid because overexpression of Sec23 is toxic. The transformants were grown to saturation at 23°C and adjusted to an OD_{600} of 0.3. Then, 5 μL of a 10-fold dilution series were spotted onto selective plates and incubated at the indicated temperatures. O/E indicates overexpression. The result shown is typical and representative of at least three independent experiments.

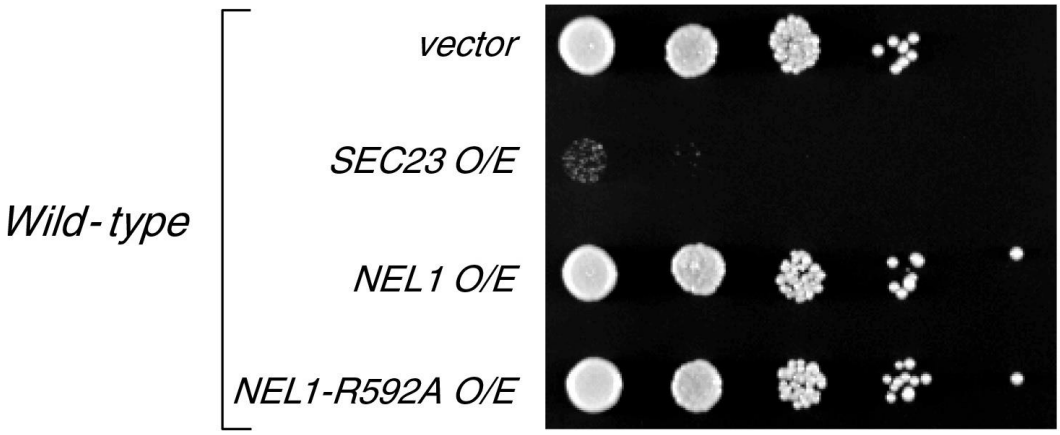

Figure 8. Nel1 overexpression does not lead to a growth defect.

Wild-type (ANY21) cells transformed with pCKY5 (*2μ* vector), pSEC23/CKY5 (*2μ SEC23*), or pNEL1/CKY5 (*2μ NEL1*) were grown to saturation at 30°C and then adjusted to an OD_{600} of 0.3. Then, 5 μL of a 10-fold dilution series were spotted onto selective plates and incubated at 30°C. O/E indicates overexpression. The result shown is typical and representative of at least three independent experiments.

4.2 Nel1 does not associate with Sec24 and its homologs

In *S. cerevisiae* and higher eukaryotes, Sec23 forms a stable complex with either Sec24 or its closely related homologs (Bi et al., 2002). I therefore determined whether Nel1 could also associate with Sec24 and its yeast homologs, Lst1 or Iss1 (Kurihara et al., 2000; Roberg et al., 1999; Shimoni et al., 2000). As revealed by a yeast two-hybrid assay, Sec23 indeed associated with Sec24, whereas no interactions were observed between Nel1 and Sec24, Lst1, or Iss1 (Fig. 9). To further confirm the two-hybrid results, I performed pull-down experiments in lysates prepared from yeast cells expressing both Nel1 tagged C-terminally with a MBP-tag (Nel1-MBP) and HA-tagged Sec24, Lst1, or Iss1. As shown in Fig. 10, I observed that Nel1-MBP was not able to pull down Sec24, Lst1, or Iss1, whereas Sec23-MBP formed complexes with Sec24 and its isoforms. Indeed, SDS-PAGE analysis of the affinity-purified Nel1-MBP fusion protein revealed that additional components did not copurify with Nel1-MBP (Fig. 11). Consistent with these findings, the residues in Sec23 involved in the intersubunit interactions between Sec24 are poorly conserved in Nel1 (Fig. 6) (Bi et al., 2002). These results suggest that, unlike Sec23, Nel1 may not associate with Sec24 and its homologs.

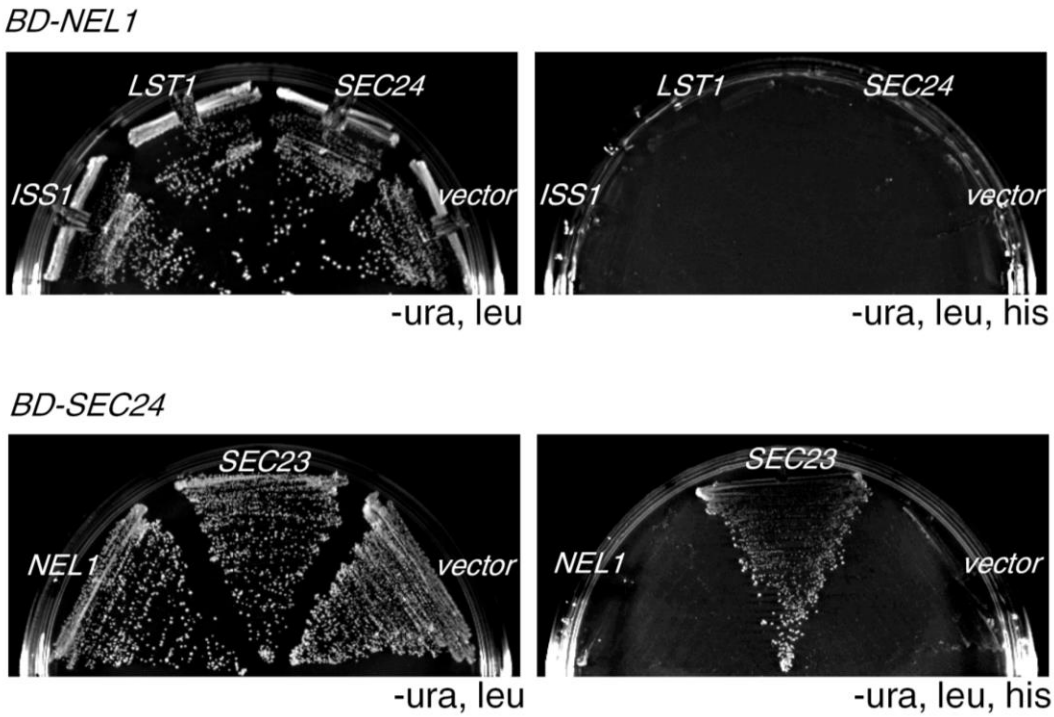

Figure 9. Nel1 does not associate with Sec24 and its homologs, as revealed by a yeast two-hybrid assay.

The PJ69-4A strain was transformed with plasmids containing the binding domain (BD)-fused Nel1 and activation domain (AD)-fused Sec24, Lst1, or Iss1, and transformants

were grown on plates lacking histidine at 30°C (upper panel). The PJ69-4A strain was transformed with plasmids containing BD-fused Sec24 and AD-fused Nel1 or Sec23, and transformants were grown on plates lacking histidine at 30°C (lower panel). Nel1 does not associate with Sec24 and its homologs, as revealed by MBP pull-down assays. Cells expressing indicated proteins were lysed and subjected to pull-down assay with the indicated MBP fusion proteins, and bound proteins were analyzed by SDS-PAGE and immunoblotting. The results shown are typical and representative of at least three independent experiments.

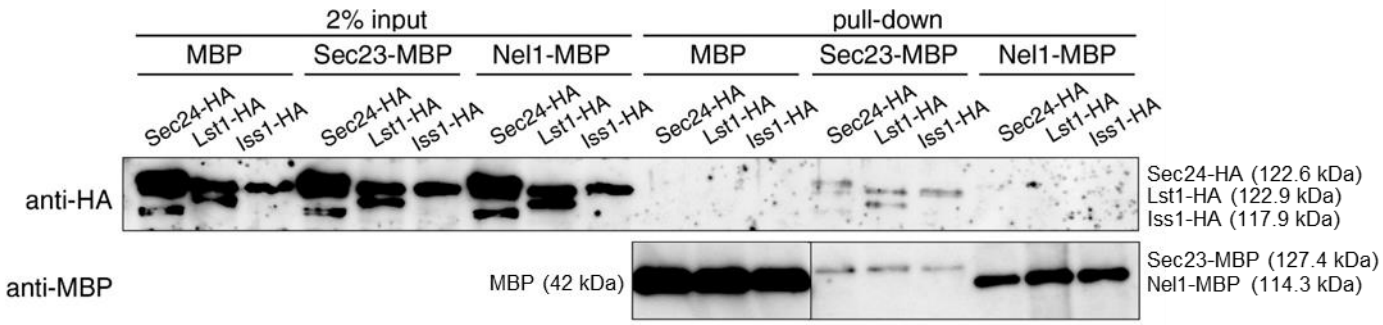

Figure 10. Nel1 does not associate with Sec24 and its homologs, as revealed by MBP pull-down assays.

Cells expressing indicated proteins were lysed and subjected to pull-down assay with the indicated MBP fusion proteins, and bound proteins were analyzed by SDS-PAGE and immunoblotting. The result shown is typical and representative of at least three independent experiments.

4.3 Nel1 has GAP activity toward Sar1

Despite the absence of a detectable interaction with Sec24 and its homologs, Nel1 contains a region with sequence homology to the C-terminal domain of Sec23, which includes a crucial arginine residue required for Sec23 GAP activity (Fig. 6) (Bi et al., 2002). The corresponding arginine residue is also conserved in Nel1 (R592), which suggests that Nel1 may also have GAP activity toward Sar1. To examine whether Nel1 affects Sar1 GTPase activity, affinity-purified Nel1-MBP was tested for GAP activity on Sar1 by using a real-time tryptophan fluorescence assay (Fig. 12) (Antonny et al., 2001; Sato and Nakano, 2005). I incubated liposomes ("major-minor mix" lipids, previously established as the optimal composition for COPII recruitment) (Matsuoka et al., 1998) preloaded with Sar1-GTP and monitored the decrease in the intrinsic tryptophan fluorescence of Sar1 that accompanies the conversion of Sar1 from the GTP state to the GDP state after the addition of Nel1-MBP or control Sec23/24 (Fig. 13). As expected, the addition of Nel1-MBP markedly accelerated the GTPase activity of Sar1. At an equal molar concentration, Nel1 was ~5-fold (in arbitrary units) more potent than Sec23/24 at promoting GTP hydrolysis on Sar1. Replacement of the arginine-592 residue of Nel1

with alanine (Nel1-R592A-MBP) virtually abolished Nel1's GAP activity, indicating the direct involvement of this residue in catalysis. I also examined the effect of Nel1-R592A overexpression on the growth of the wild-type strain and observed no detectable alternation in growth rate (Fig. 8), suggesting that Nel1 GAP activity is not directly involved in normal cell growth.

I next determined whether the GAP activity of Nel1 could be further accelerated by Sec13/31, as has been observed with Sec23 (Antonny et al., 2001). However, the presence of Sec13/31 did not substantially influence the GAP activity of Nel1 (Fig. 14). Assembly of the COPII coat proceeds in a stepwise manner by the recruitment of Sar1-GTP, which binds to the lipid surface, followed by association of Sec23/24 and Sec13/31. This process has been reconstituted *in vitro* using synthetic liposomes (Matsuoka et al., 1998). I tested the ability of Nel1 to bind to liposomes loaded with Sar1 and whether it could in turn recruit Sec13/31 in this reconstituted system. Liposomes were incubated with different combinations of the COPII coat proteins as indicated in Fig. 15 (upper panel), followed by floatation on a sucrose density gradient. Similar to Sec23/24, Nel1 bound to these liposomes in a Sar1- and GMP-PNP-dependent manner, but the

subsequent recruitment of Sec13/31 was not observed. Therefore, the complete loss of the ability of Sec13/31 to stimulate the GAP activity of Nel1 is likely to be due to the fact that Nel1 is not active in the recruitment of Sec13/31. Consistent with these findings, the residues in Sec23 involved in the intersubunit contacts with Sec31 are poorly conserved in Nel1 (Fig. 6) (Bi et al., 2007). To compare the relative affinities of Sec23 and Nel1 for Sar1, I quantified the binding efficiencies of these two proteins to Sar1 in Fig. 15 (upper panel). The binding levels relative to the amount of membrane-bound Sar1 were similar for both Sec23 (0.0037 ± 0.0018) and Nel1 (0.0034 ± 0.00043) (Fig. 15, lower panel), indicating that the Nel1 has roughly equal affinity for Sar1 as Sec23. I also confirmed that Nel1-R592A-MBP can bind to Sar1-GMP-PNP, ensuring that this mutant protein was properly folded (Fig. 16). Furthermore, the fact that Nel1-R592A-MBP can bind Sar1, but exhibits no GAP activity excludes the possibility that tryptophan residues in Nel1 somehow contribute to the change in fluorescence that occurs upon incubation with Sar1-GTP, as observed in Fig. 13. I concluded from these kinetic and biochemical results that Nel1 has some role in the regulation of Sar1 GTPase activity but may have a function distinct from that of Sec23 as a subunit of the COPII vesicle coat.

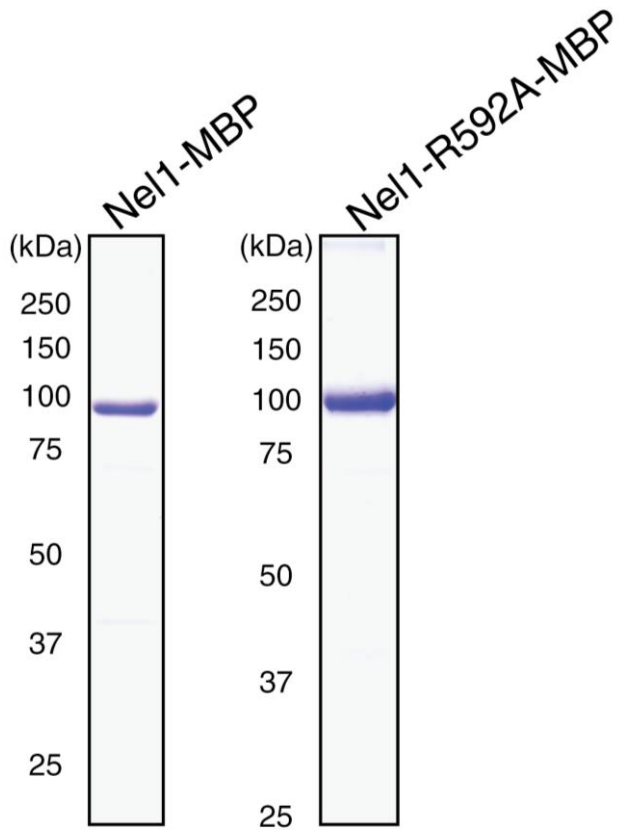

Figure 11. Nel1-MBP and Nel1-R592A-MBP were purified from yeast cells.

Proteins from YHP500 cells expressing Nel1-MBP or Nel1-R592A-MBP were purified by amylose resin, and they were separated by SDS-PAGE followed by staining with Coomassie brilliant blue.

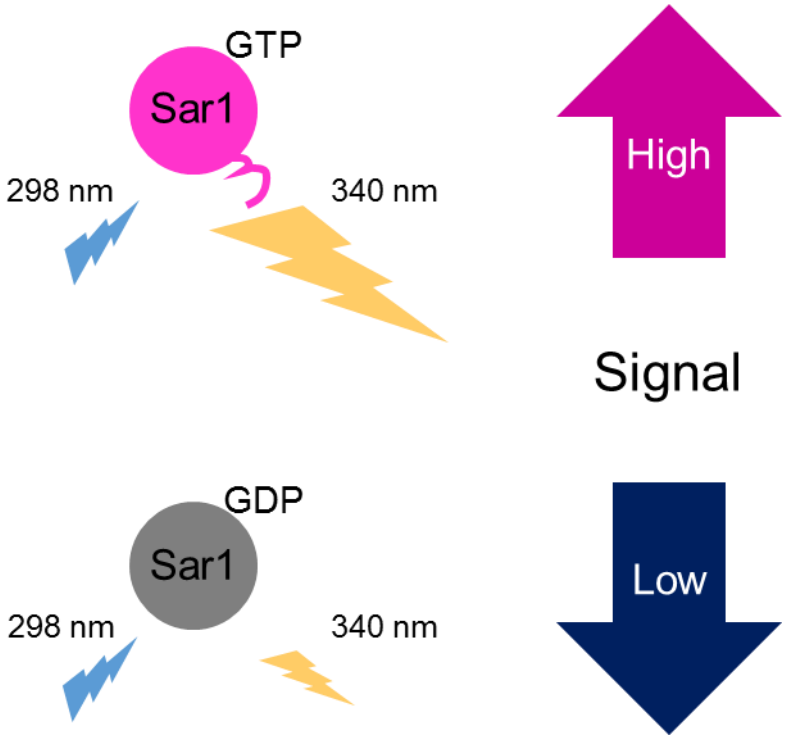

Figure 12. Schematic diagram of tryptophan fluorescent measurement.

Conformational change between Sar1-GTP and Sar1-GDP could be monitored by measuring the intrinsic tryptophan fluorescence of Sar1. Sar1-GTP shows higher fluorescence than Sar1-GDP.

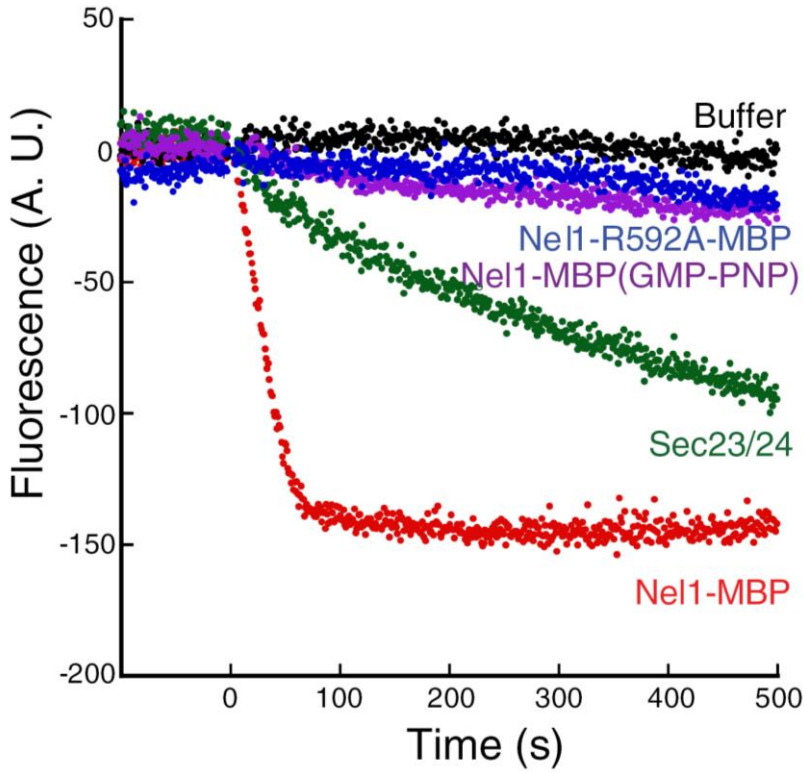

Figure 13. Nel1 accelerates GTP hydrolysis by Sar1.

The reaction initially contained liposomes (100 µg/mL), Sar1 (800 nM), and GTP or GMP-PNP (0.1 mM). After preincubation, Nel1-MBP, Nel1-R592A-MBP, or Sec23/24 (15 nM) were added at 0 sec. Transition of Sar1 from the GTP-bound to the GDP-bound state was monitored by tryptophan fluorescence of Sar1 at 340 nm. The results shown are typical and representative of at least three independent experiments.

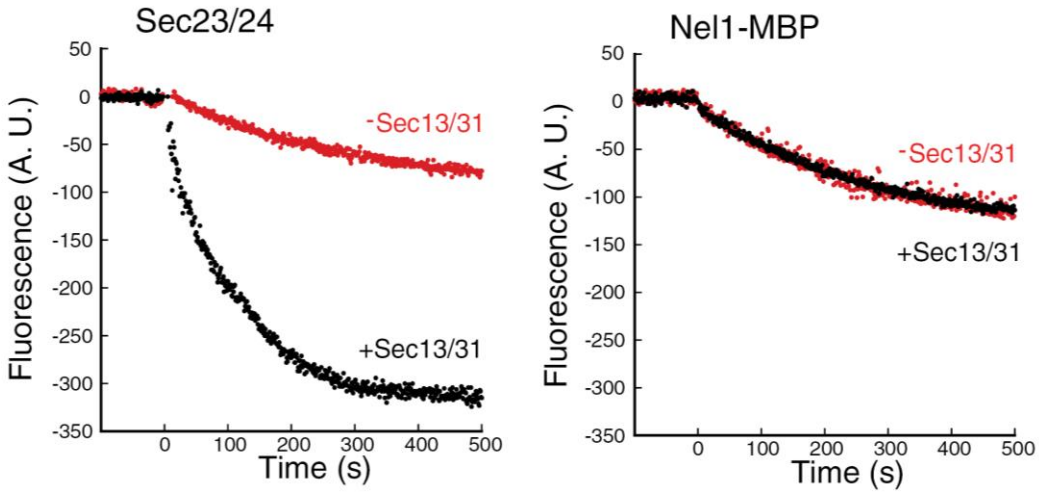

Figure 14. Sec13/31 does not stimulate Nel1-mediated GAP activity on Sar1.

The reaction initially contained liposomes (100 µg/mL), Sar1 (800 nM), and GTP (0.1 mM). After preincubation, Sec23/24 (15 nM) and Sec13/31 (22.5 nM) (left panel) or Nel1-MBP (5 nM) and Sec13/31 (5 nM) (right panel) were added at 0 sec, and the Sar1-GTP to Sar1-GDP transition was monitored by tryptophan fluorescence of Sar1 at 340 nm. The results shown are typical and representative of at least three independent experiments.

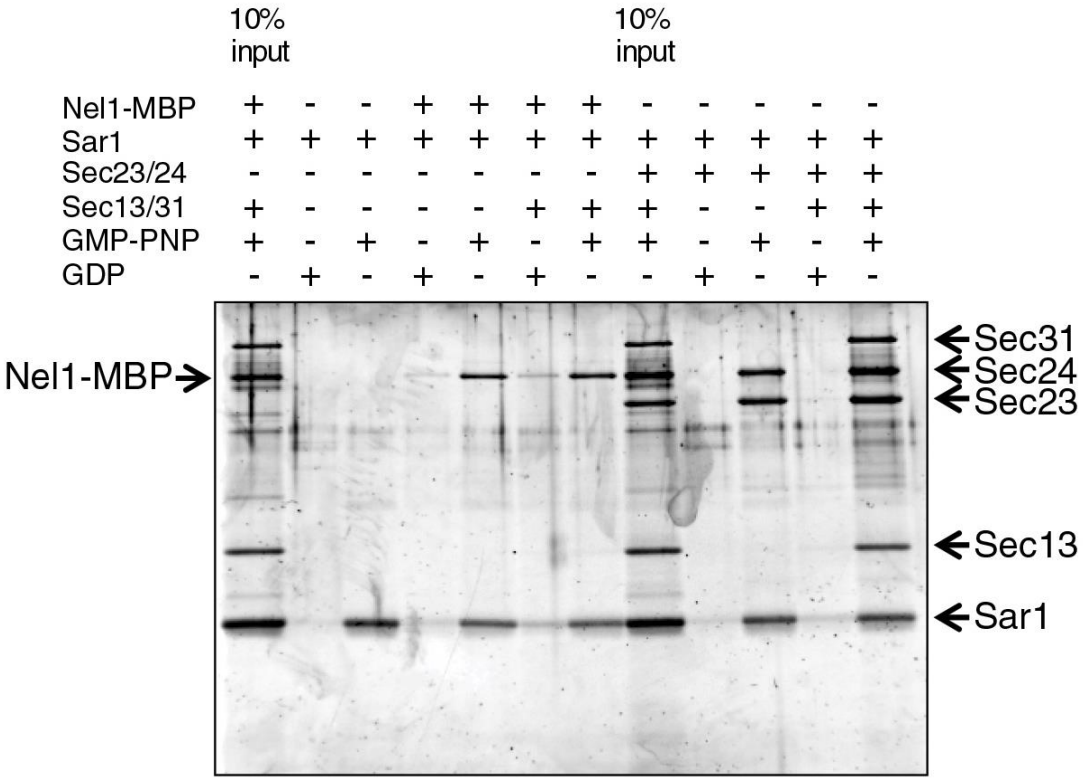
10% input
10% input
Nel1-MBP + - - + + + + - - - - -
Sar1 + + + + + + + + + + + +
Sec23/24 - - - - - - - + + + + +
Sec13/31 + - - - - + + + - - + +
GMP-PNP + - + - + - + + - + - +
GDP - + - + - + - - + - + -
Nel1-MBP
Sec31
Sec24
Sec23
Sec13
Sar1

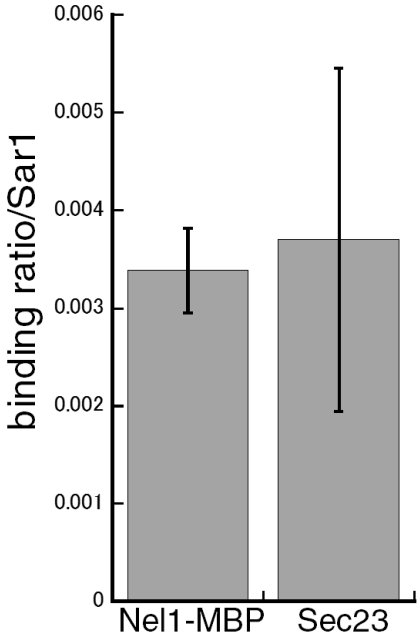
binding ratio/Sar1
0.006
0.005
0.004
0.003
0.002
0.001
0
Nel1-MBP
Sec23

Figure 15. Liposome-binding assays of COPII proteins with Nel1.

Sar1 (800 nM), Sec13/31 (200 nM), Nel1-MBP or Sec23/24 (120 nM) were incubated with GDP or GMP-PNP (0.1 mM) in the presence of synthetic liposomes (100 µg/mL), and subjected to flotation on a sucrose density gradient. Float fractions were then subjected to SDS-PAGE and stained with SYPRO Orange (upper panel). The result shown is typical and representative of at least three independent experiments. Quantification of the binding efficiencies of Sec23 and Nel1-MBP for Sar1. The band intensities of Sec23 or Nel1 in (upper panel) were normalized to those of Sar1, and the values of Sar1 bound Sec23 (or Nel1-MBP)/total input Sec23 (or Nel1-MBP) were calculated. The means and standard deviations are shown in the graph. These results were verified by applying Student's t-test. p value was > 0.1 (lower panel).

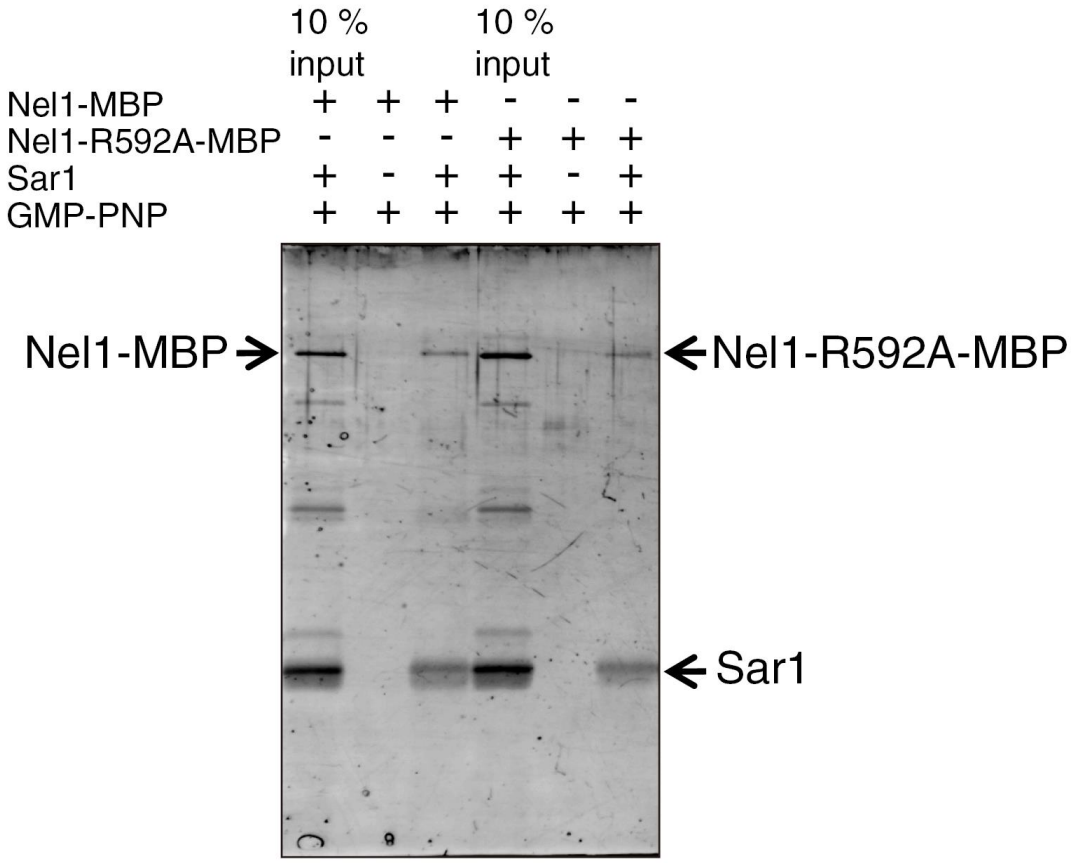

Figure 16. Liposome-binding assays of Nel1-R592A.

Sar1 (800 nM), Nel1-MBP (120 nM) or Nel1-R592A-MBP (120 nM) were incubated with GMP-PNP (0.1 mM) in the presence of synthetic liposomes (100 µg/mL) and subjected to flotation as in (Fig. 15). The result shown is typical and representative of at least three independent experiments.

4.4 Chromosomal disruption of NEL1 in combination with *sar1D32G* mutation exhibits a slow growth phenotype

To obtain evidence of a functional relationship between Sar1 and Nel1 *in vivo*, I examined genetic interactions between the genes (Fig. 17-20). To this end, the temperature-sensitive *sar1D32G* allele was combined with the *nel1*Δ mutation, and the ability of this mutant to grow at the permissive temperature (23°C) was assessed. The single *nel1*Δ mutant cells grew identically to wild-type cells, whereas the growth of the *sar1D32G* mutant was much slower even at the permissive temperature as previously reported (Fig. 17) (Yamanushi et al., 1996). The growth rate was further impaired in the *sar1D32G*/*nel1*Δ double mutant (Fig. 18). This growth defect of the *sar1D32G*/*nel1*Δ strain could be restored by introduction of a plasmid carrying the *NEL1* gene (Fig. 19). These observations indicate that combining the *sar1D32G* and *nel1*Δ mutations causes a synthetic growth defect and thus provide strong genetic support for a possible functional link between Sar1 and Nel1. I also confirmed that the tagged versions of Nel1 (Nel1-13myc, Nel1-GFP, and Nel1-mCherry) were fully functional by observing complementation of the growth defect of a *sar1D32G*/*nel1*Δ strain (Fig. 20).

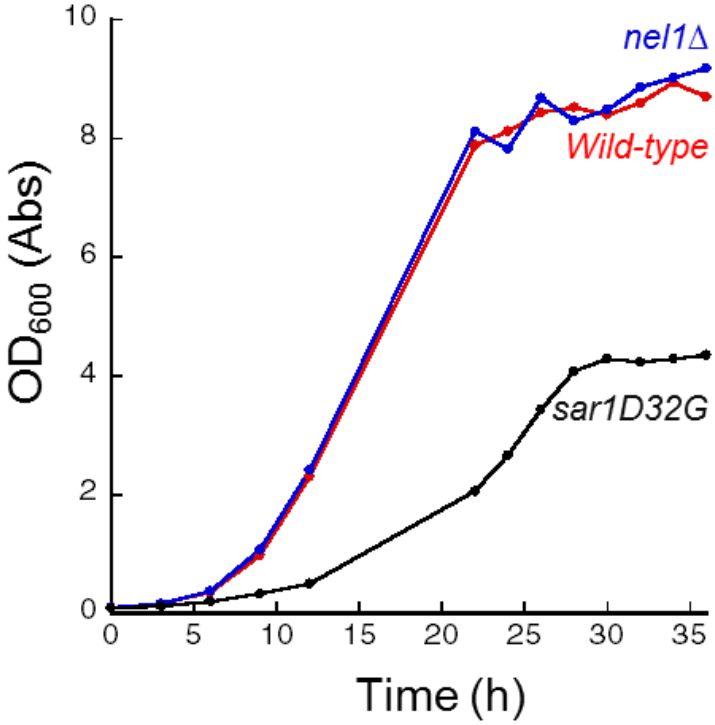

Figure 17. Growth phenotype of the *nel1*Δ strain.

Wild-type (TOY221), *nel1*Δ (CKY2), and *sar1D32G* (TOY223) cells were cultured at 23°C overnight and adjusted to an OD_{600} of 0.1 in YPD medium Then the cultures were analyzed for growth at 23°C over time by absorbance at 600 nm. The results shown are typical and representative of at least three independent experiments.

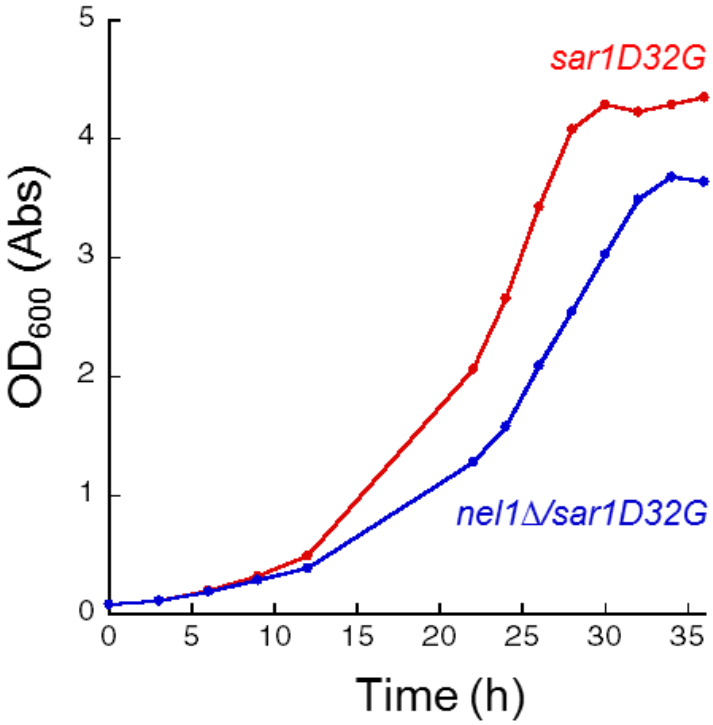

Figure 18. The *sar1D32G*/*nel1*Δ double mutant has a synthetic growth defect.

The *sar1D32G* (TOY223) and *sar1D32G*/*nel1*Δ (CKY3) cells were analyzed as in (Fig. 17). The results shown are typical and representative of at least three independent experiments.

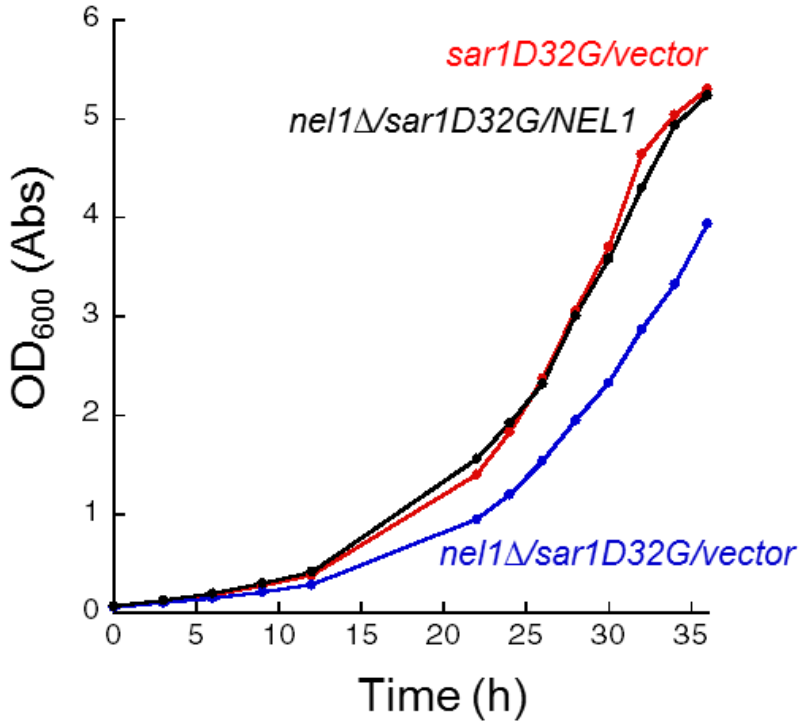

Figure 19. The *sar1D32G/nel1*Δ synthetic growth is rescued by plasmid expressing Nel1.

The *sar1D32G* (TOY223) and *sar1D32G/nel1*Δ (CKY3) cells carrying the indicated plasmids were analyzed as in (Fig. 17). The results shown are typical and representative of at least three independent experiments.

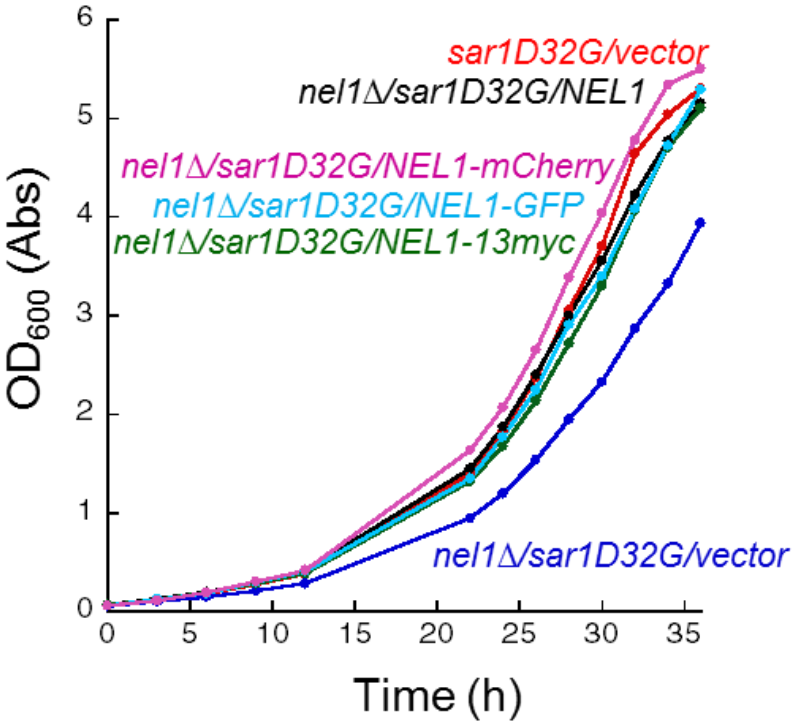

Figure 20. The *sar1D32G/nel1*Δ synthetic growth is rescued by plasmid expressing tagged versions of Nel1.

The *sar1D32G* (TOY223) and *sar1D32G/nel1*Δ (CKY3) cells carrying the indicated plasmids were analyzed as in (Fig. 17). The results shown are typical and representative of at least three independent experiments.

4.5 Subcellular localization of Nel1

COPII coat proteins, including Sec23, are predominantly localized to punctate structures at ERES on the ER membrane (Rossanese et al., 1999; Shindiapina and Barlowe, 2010). I next sought to determine the subcellular localization of Nel1-GFP expressed under its own promoter, but the expression was found to be below the limit of detection. Nel1 fusions that contained two or even three tandem repeats of the GFP moiety showed the same result, suggesting that this protein is expressed at much lower levels than Sec23. I therefore examined the localization of overexpressed Nel1-GFP or Nel1-mCherry (Fig. 21, upper panel and Fig. 22). In sharp contrast with its homolog Sec23, the fluorescence for Nel1 was diffusely localized throughout the cytosol, and I could not observe any ERES-like punctate structures. In addition, Nel1 was also found in the nucleus, as evidenced by its colocalization with the nuclear marker Htb1-GFP (Michelsen et al., 2006; Zou et al., 2012), and in most cells the nuclear signal was slightly stronger (signal ratio of nucleus/cytosol=1.2 ± 0.28) (Fig. 21, lower panel). To evaluate whether the localization pattern of overexpressed Nel1 corresponds to that of endogenous Nel1, I used subcellular fractionation to examine the localization of a C-terminally

13myc-tagged version of Nel1 (Nel1-13myc) expressed from its own promoter (Fig. 23). Cells expressing Nel1-13myc were converted into spheroplasts and homogenized, and the extracts were separated by centrifugation into low-speed supernatant (S13) and low-speed pellet (P13) fractions (Fig. 5D) (Vida et al., 1990). Under these conditions, the ER membrane marker Dpm1 and the nuclear marker Nop1 were found solely in the P13 fraction. The soluble marker protein Pgk1 was detected exclusively in the S13 fraction, indicating complete cell lysis. A significant portion of Sec23 was recovered in the S13 fraction (percent ratio of P13/total = 62.3 ± 3.3%), but it was also present in the P13 fraction (percent ratio of P13/total = 37.7 ± 3.3%), which reflected the amount of Sec23 localized to the ERES (Fig. 23). In contrast, Nel1-13myc was found to be predominantly localized to the S13 fraction (percent ratio of P13/total = 87.1 ± 10.0%), and ~3-fold less Nel1-13myc compared to that of Sec23 was recovered in the P13 fraction (percent ratio of P13/total = 12.9 ± 10.0%) (Fig. 23), which correlates with the localization of the overexpressed Nel1-mCherry I observed via fluorescence microscopy (Fig. 21, upper panel and Fig. 22). Together, these findings indicate that Nel1 is predominantly a cytosolic protein and does not accumulate at ERES.

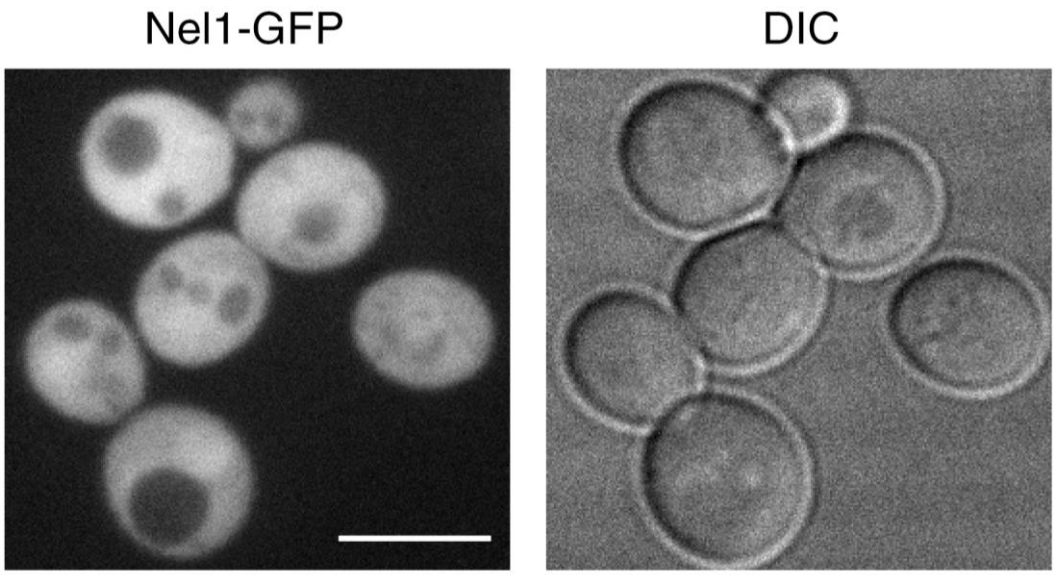
Nel1-GFP
DIC

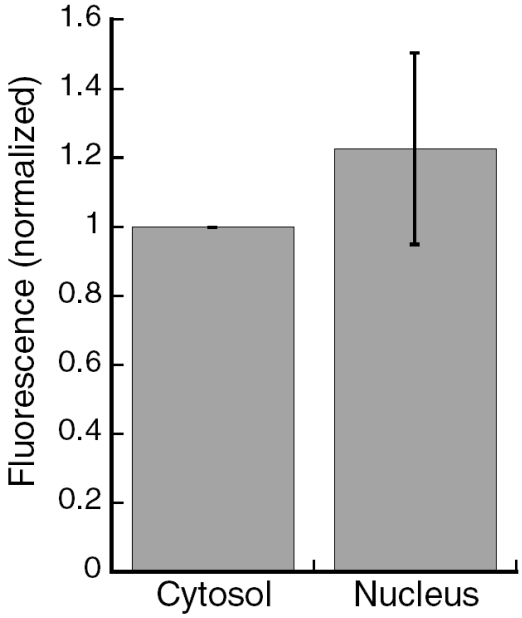
Fluorescence (normalized)
1.6
1.4
1.2
1
0.8
0.6
0.4
0.2
0
Cytosol
Nucleus

Figure 21. Live cell imaging of Nel1-GFP.

The cells expressing Nel1-GFP were grown to mid-log phase and observed by confocal microscopy (upper panel). Scale bar, 5 µm. Quantification of Nel1 accumulation in the nucleus. The fluorescence intensity of Nel1-GFP was measured, and the ratio of nuclear fluorescence to cytosolic signal was calculated for each cell (normalized relative to the cytosol). The mean and standard deviation are shown in the graph. I counted 80 cells (lower panel). The raw data of these results were verified by applying Student's t-test. p value was $0.05 < p < 0.10$.

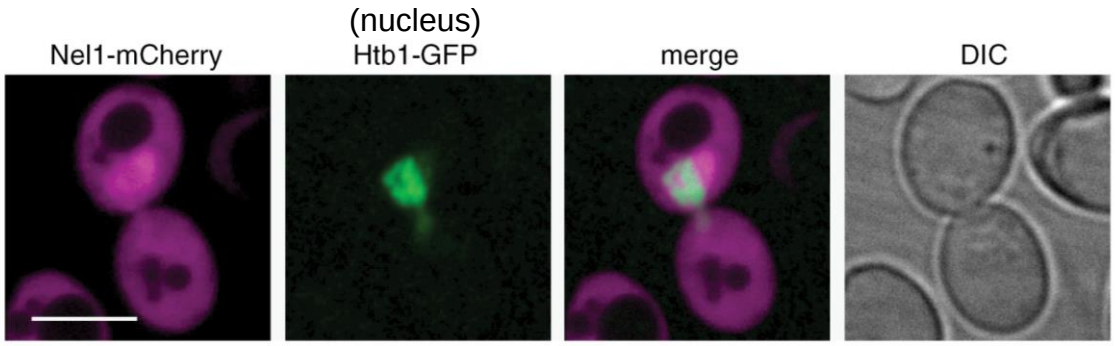

Figure 22. Nel1 is localized in the cytosol and the nucleus.

The cells expressing Htb1-GFP and Nel1-mCherry were grown to mid-log phase and observed by confocal microscopy. Scale bar, 5 µm.

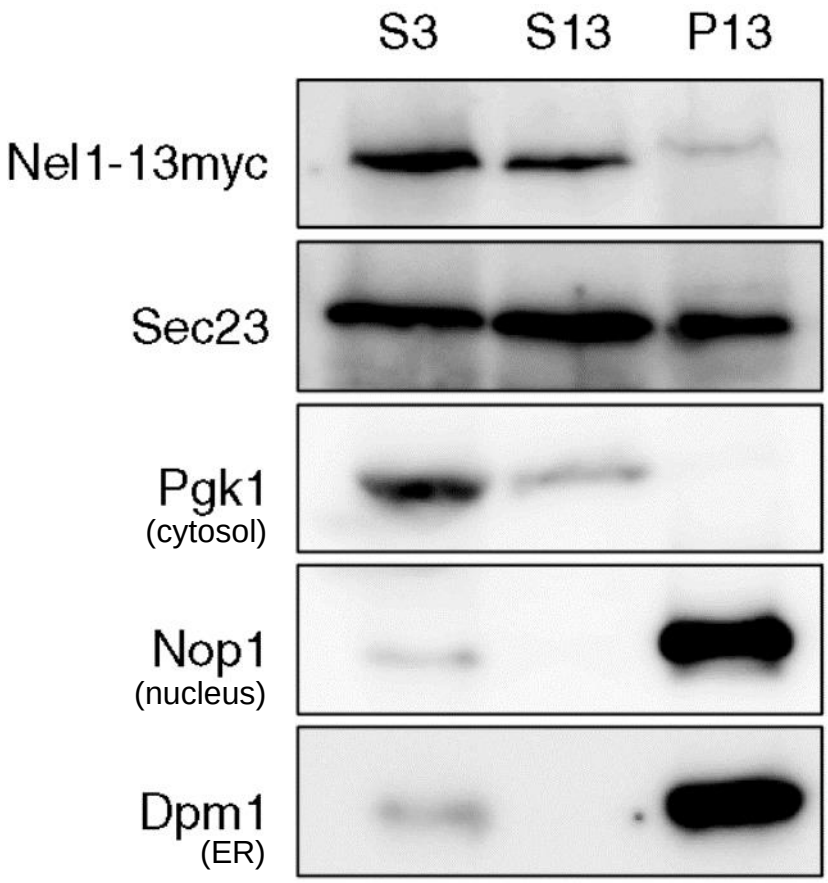

Figure 23. Subcellular fractionation analyses of Nel1 and Sec23.

The CKY1 cells expressing Nel1-13myc were grown to mid-log phase, converted to spheroplasts, homogenized, and centrifuged at 13,000 × *g*. The total homogenate (S3), supernatant (S13), and pellet (P13) fractions were analyzed by SDS-PAGE and immunoblotting. The results shown are typical and representative of at least three independent experiments.

Chapter V

Discussion

Sec23 is commonly known as a component of the COPII coat, and also as a GAP for Sar1 that regulates COPII assembly. Here, I showed that the Sec23 homolog Nel1 also has Sar1-GAP activity, but lacks the ability to function as a subunit of the COPII coat. Whether the presence of a Nel1-like molecule is specific to *S. cerevisiae* or more widespread among other organisms is currently unclear. However, since several alternative splice variants of the Sec23 gene have been predicted to exist in many higher eukaryotes (Aceview, NCBI) (Table 2.), it is possible that one of these variants has the potential to encode a protein with properties similar to those of Nel1.

At the subcellular level, Nel1 was found to be predominantly localized throughout the cytosol, which permits the activation of Sar1 GTPase on the ER membrane. Although overexpression of Sec23 alone has been shown to impair cell growth, I was unable to detect any apparent growth defect when Nel1 was overexpressed. This is likely because Nel1 does not associate with any of the COPII coat components; therefore, it may not compete for COPII coat assembly. In fact, the fluorescence signal of Nel1-mCherry was not concentrated at ERES. To our knowledge, failure to localize at ERES has not previously been described for Sec23 or any of its homologs found in other species (Esaki

et al., 2006; Orci et al., 1991; Paccaud et al., 1996; Yang et al., 2005). Although there remains the possibility that the overexpression of Nel1 might affect its normal intracellular localization pattern, my data indicate that Nel1 is also localized in the nucleus. The size limit for passive diffusion through the nuclear pore complex is approximately ~40 kDa (Terry et al., 2007); therefore, Nel1-mCherry (99 kDa), as well as endogenous Nel1 (72 kDa), are considered too large to diffuse freely into the nucleus. Thus, a functional nuclear localization signal (NLS) would be required for the active transport of Nel1 into the nucleus; however, no conventional NLS is evident in the Nel1 sequence. The exact sequences responsible for nuclear targeting of Nel1 remain to be established.

I further showed here that Nel1 interacts biochemically with Sar1 and acts as a GAP to stimulate GTPase activity. The demonstration that Nel1 binds to the membrane via the GTP-bound form of Sar1 and catalyzes its inactivation implies that Nel1 modulates the activity of Sar1 on the membrane. On the basis of my result that a subpopulation of Nel1 shuttles to the nucleus, it might be possible that Nel1 has a physiological function there. A fraction of Sar1 might also be localized inside the nucleus

because endogenous Sar1 (at 21.5 kDa) is small enough to diffuse into the nucleus without requiring a functional NLS. Although my genetic analysis of the *nel1*Δ *sar1D32G* double mutant suggests a functional link between Nel1 and Sar1 *in vivo*, further studies will be needed to determine the precise mechanistic relationship between Sar1 and nuclear-localized Nel1.

To summarize, I identified Nel1 as a novel homolog of Sec23 that has genetic and biochemical interactions with Sar1 in *S. cerevisiae*. The function of Nel1 is currently unknown. However, considering its considerably lower level of expression than that of Sec23, I think it is unlikely that Nel1 functions as a structural component of the vesicle coat machinery. Instead, I propose that Nel1 functions as a signaling molecule. Further investigation may provide insight into the physiological relevance of Sar1/Nel1 function in the cells (Fig. 24).

Table 2. The examples of Sec23 homologs.

S. cerevisiae	*P. pastoris*	*D. rerio*	*H. sapiens*	*A. thaliana*
Sec23	Sec23	Sec23a	Sec23A	At3g23660
Nel1	Shl23	Sec23b	Sec23B	At1g05520
				At5g43670
				At4g14160
				At2g21630
				At4g01810
				At2g27460

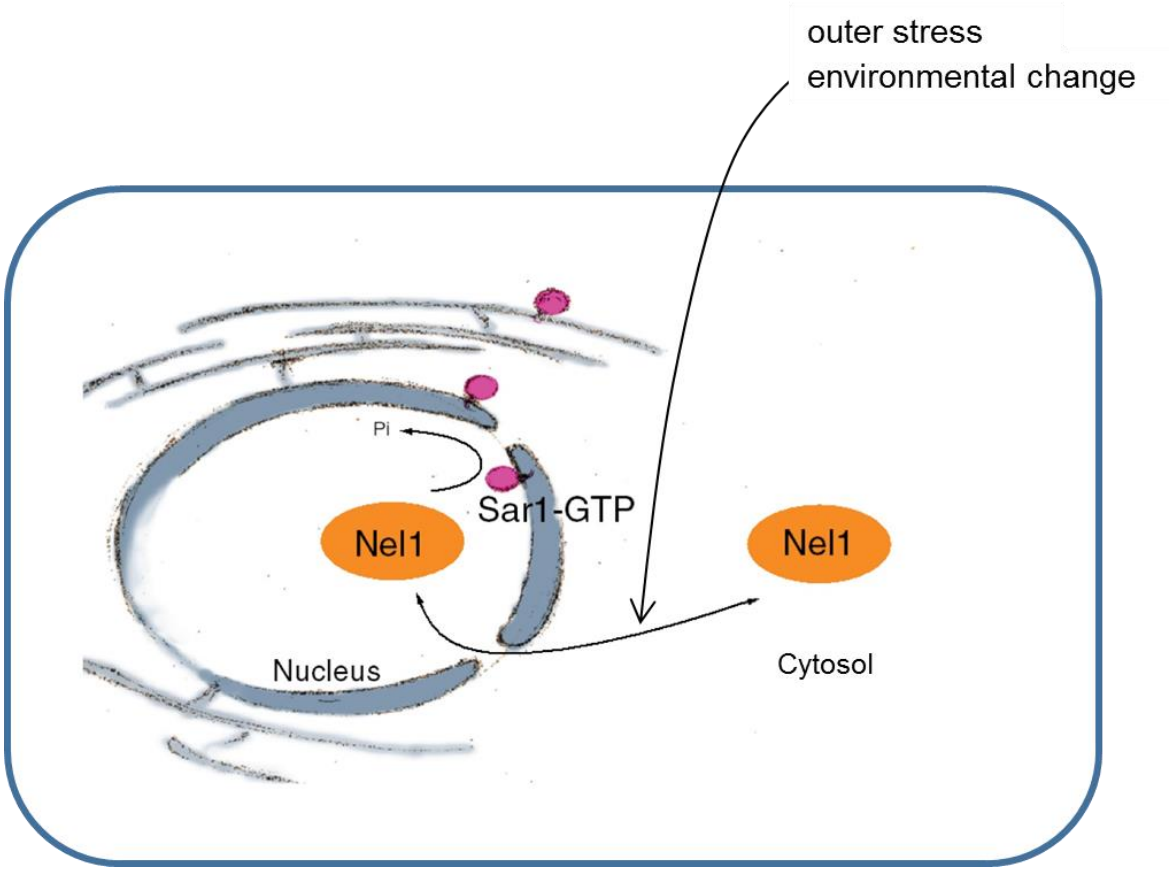

Figure 24. Schematic model of Nel1 function.

Nel1 may shuttle between cytosol and nucleus in response to outer signal.

Chapter VI

General Discussion

Although numerous aspects of COPII vesicle formation have been unveiled through the past decades, several questions remain unanswered. One of the important questions is how cells regulate the amount or balance of transport. The streaming of proteins and lipids changes in response to varying environmental conditions. Therefore, the amount and timing of generating transport carriers have to be regulated strictly. Moreover, the balance of anterograde and retrograde transport is essential for retaining organelles, as well as for appropriate secretion. The most upstream initiator of COPII carrier formation known thus far is Sec12. However, no regulator of Sec12 has been discovered yet. Some accessory proteins are known to modulate COPII carrier formation, but complex combinations of these proteins are not fully understood (D'Arcangelo et al., 2013). Under stress conditions, unfolded protein response also regulates ER–Golgi transport (Amodio et al., 2009; Farhan et al., 2008; Higashio and Kohno, 2002; Sato et al., 2002). Precise analysis and integrated information on cell homeostasis are necessary to solve this complex and challenging question.

The next important question is, do COPII vesicles exist as real structures in the cell? *In vitro* reconstitution systems generate small membrane vesicles (Matsuoka et al., 1998). However, COPII–coated vesicles were not found in yeast and certain plant cells in some studies (Robinson et al., 2007; West et al., 2011). The COPII machineries are highly conserved across eukaryotes, but distinct membrane vesicles were not detected in yeast cells. Moreover, in mammalian cells, large cargos, for example procollagen, could not be packaged into small vesicles, implying that there have to be large intermediate carriers between the ER and Golgi apparatus (Malhotra and Erlmann, 2011). Non-vesicular intermediates like tubular structures might be responsible for the transport pathway from the ER (English and Voeltz, 2013; Glick and Nakano, 2009). A recent study showed that the Golgi apparatus approaches and captures cargoes at the ERES directly (Kurokawa et al., 2014). However, the inability to detect small vesicles in the cell might be due to their transient existence or technical inadequacies in available detection systems. Thus, there is no direct evidence that supports the vesicular model or the non-vesicular model.

Some interesting factors that function as regulators for Sar1 GTPase warrant discussion. In the early stages of COPII vesicle formation, Sed4 is a mysterious player (Hardwick et al., 1992; Kodera et al., 2011). Sed4 and Sec12 have similar catalytic regions, but their functions are completely the opposite. Sec12 is a GEF for Sar1, but Sed4 promotes Sar1 GTP hydrolysis (Kodera et al., 2011). How does Sed4 stimulate Sar1 GTPase activity? There could be a yet undiscovered mechanism that accelerates Sar1 GTP hydrolysis, different from that of conventional GAP. Sed4 has been reported only in *S. cerevisiae*. In other eukaryotes, Sec12 could have a similar function as Sed4. Otherwise, there might be a functional alternative. Sed4 interacts with Sec16 at the genetic and physical level. However, the implications of these interactions are not clear. Sed4 stimulates the GTPase activity of Sar1, while Sec16 inhibits the activity (Kung et al., 2012; Yorimitsu and Sato, 2012). What would happen when they interact in the cell is not known. In addition, why are Sed4 and Sar1 distributed throughout the ER membrane? Why are they not concentrated at the ERESs? Sar1 may have another function distinct from making COPII carriers, and it is interesting to speculate that Sed4 inhibits

COPII carrier formation by releasing Sar1 from the membrane regions other than the ERES.

In this study, I report on a novel Sar1 GAP, Nel1. Nel1 has strong GAP activity towards Sar1, and Nel1 and Sar1 interact at the genetic level. However, the physiological roles of Nel1 are not clear. Does Nel1 have any relation with COPII carriers or vesicular transport? My data suggest that Nel1 does not function at the ERES as a COPII coat component like Sec23. However, it can be speculated that Nel1 associates with a regulating process of vesicular transport in certain situations, or that it prevents COPII vesicle formation at a site where COPII vesicles should not to be generated (for instance, in the nucleus) by accelerating Sar1 GTP hydrolysis and releasing Sar1 from the membrane. Otherwise, the idea that Nel1 has functions other than vesicular transport is also plausible (Fig. 25). The latter idea also suggests that Sar1 could have a hidden function associated with Nel1. My new findings highlight the novel function of Sar1 and the importance of its regulatory factors.

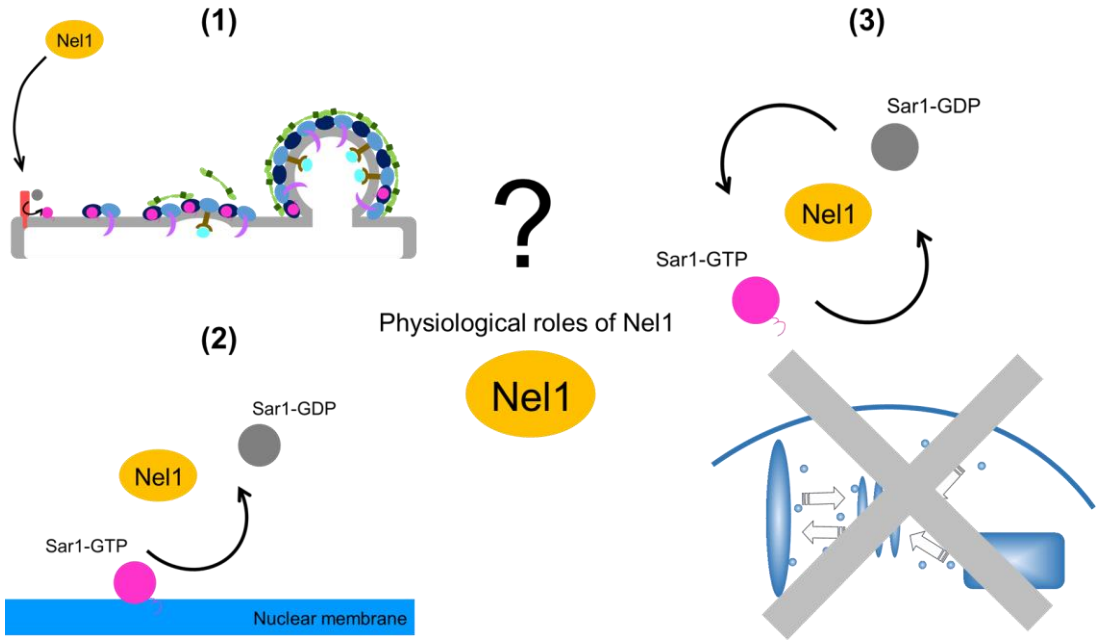

Figure 25. Possibilities of Nel1 physiological functions.

Nel1 may associate with a regulating process of vesicular transport in certain situations (1), or prevent COPII vesicle formation at a site where COPII vesicles should not to be generated by accelerating Sar1 GTP hydrolysis and releasing Sar1 from the membrane (2). Otherwise, the idea that Nel1 has functions other than vesicular transport is also plausible (3).

Recently, COPII-related proteins have been shown to be involved in processes different from the transport system. For example, COPII-related genes are reported to be involved in ER-associated degradation. Early sec proteins work through the process to segregate unfolded proteins into specialized sites on the ER membrane (Kakoi et al., 2013). The relationship between ER-Golgi transport and autophagy is rapidly becoming a hot topic in the field of cell biology. Some transport-related proteins have been reported to be necessary for autophagy (Hamasaki et al., 2003; Ishihara et al., 2001; Tan et al., 2013). Moreover, the formation of autophagosomes might be occurring very close to the ERES (Graef et al., 2013). Perhaps Nel1 is involved in these multiple processes to maintain cell homeostasis and respond to environmental conditions.

Finally, I comment on a fundamental question. What is an organelle? In this last decade, some organelles and their intermediates have been reported to undergo maturation processes (Glick and Nakano, 2009). The transport system itself is important for their maintenance, and there also must be recognition systems to identify each organelle. Are there concrete boundaries between organelles? Could it be possible that

many organelles are interconnected and comprise a giant membrane structure as a single unit, with distinct areas for separate functions? Our commonly accepted conceptual images of organelles might now be shaken by current findings. Unveiling the sophisticated coordination mechanisms of membrane dynamics would be interesting and compelling in this field.

References

Amodio, G., Renna, M., Paladino, S., Venturi, C., Tacchetti, C., Moltedo, O., Franceschelli, S., Mallardo, M., Bonatti, S., and Remondelli, P. (2009). Endoplasmic reticulum stress reduces the export from the ER and alters the architecture of post-ER compartments. The international journal of biochemistry and cell biology *41*, 2511-2521.

Antonny, B., Madden, D., Hamamoto, S., Orci, L., and Schekman, R. (2001). Dynamics of the COPII coat with GTP and stable analogues. Nature cell biolgy *3*, 531-537.

Balch, W.E., Dunphy, W.G., Braell, W.A., and Rothman, J.E. (1984). Reconstitution of the transport of protein between successive compartments of the Golgi measured by the coupled incorporation of N-acetylglucosamine. Cell *39*, 405-416.

Barlowe, C., d'Enfert, C., and Schekman, R. (1993). Purification and characterization of SAR1p, a small GTP-binding protein required for transport vesicle formation from the endoplasmic reticulum. The journal of biological chemistry *268*, 873-879.

Barlowe, C., Orci, L., Yeung, T., Hosobuchi, M., Hamamoto, S., Salama, N., Rexach,

M.F., Ravazzola, M., Amherdt, M., and Schekman, R. (1994). COPII: a membrane coat formed by Sec proteins that drive vesicle budding from the endoplasmic reticulum. Cell *77*, 895-907.

Barlowe, C., and Schekman, R. (1993). SEC12 encodes a guanine-nucleotide-exchange factor essential for transport vesicle budding from the ER. Nature *365*, 347-349.

Barlowe, C.K., and Miller, E.A. (2013). Secretory protein biogenesis and traffic in the early secretory pathway. Genetics *193*, 383-410.

Belden, W.J., and Barlowe, C. (2001). Role of Erv29p in collecting soluble secretory proteins into ER-derived transport vesicles. Science *294*, 1528-1531.

Bi, X., Corpina, R.A., and Goldberg, J. (2002). Structure of the Sec23/24-Sar1 pre-budding complex of the COPII vesicle coat. Nature *419*, 271-277.

Bi, X., Mancias, J.D., and Goldberg, J. (2007). Insights into COPII coat nucleation from the structure of Sec23. Sar1 complexed with the active fragment of Sec31. Developmental cell *13*, 635-645.

Bonifacino, J.S., and Glick, B.S. (2004). The mechanisms of vesicle budding and fusion. Cell *116*, 153-166.

Boyadjiev, S.A., Fromme, J.C., Ben, J., Chong, S.S., Nauta, C., Hur, D.J., Zhang, G., Hamamoto, S., Schekman, R., Ravazzola, M., *et al.* (2006). Cranio-lenticulo-sutural dysplasia is caused by a SEC23A mutation leading to abnormal endoplasmic-reticulum-to-Golgi trafficking. Nature genetics *38*, 1192-1197.

Brandizzi, F., and Barlowe, C. (2013). Organization of the ER-Golgi interface for membrane traffic control. Nature reviews molecular cell biology *14*, 382-392.

Bue, C.A., and Barlowe, C. (2009). Molecular dissection of Erv26p identifies separable cargo binding and coat protein sorting activities. The journal of biological chemistry *284*, 24049-24060.

D'Arcangelo, J.G., Stahmer, K.R., and Miller, E.A. (2013). Vesicle-mediated export from the ER: COPII coat function and regulation. Biochimica et biophysica acta *1833*, 2464-2472.

English, A.R., and Voeltz, G.K. (2013). Endoplasmic reticulum structure and interconnections with other organelles. Cold spring harbor perspectives in biology *5*, a013227.

Esaki, M., Liu, Y., and Glick, B.S. (2006). The budding yeast *Pichia pastoris* has a novel

Sec23p homolog. FEBS letters *580*, 5215-5221.

Espenshade, P., Gimeno, R.E., Holzmacher, E., Teung, P., and Kaiser, C.A. (1995). Yeast SEC16 gene encodes a multidomain vesicle coat protein that interacts with Sec23p. The journal of cell biology *131*, 311-324.

Farhan, H., Weiss, M., Tani, K., Kaufman, R.J., and Hauri, H.P. (2008). Adaptation of endoplasmic reticulum exit sites to acute and chronic increases in cargo load. The EMBO journal *27*, 2043-2054.

Futai, E., Hamamoto, S., Orci, L., and Schekman, R. (2004). GTP/GDP exchange by Sec12p enables COPII vesicle bud formation on synthetic liposomes. The EMBO journal *23*, 4146-4155.

Gimeno, R.E., Espenshade, P., and Kaiser, C.A. (1995). SED4 encodes a yeast endoplasmic reticulum protein that binds Sec16p and participates in vesicle formation. The journal of cell biology *131*, 325-338.

Gimeno, R.E., Espenshade, P., and Kaiser, C.A. (1996). COPII coat subunit interactions: Sec24p and Sec23p bind to adjacent regions of Sec16p. Molecular biology of the cell *7*, 1815-1823.

Glick, B.S., and Nakano, A. (2009). Membrane traffic within the Golgi apparatus. Annual review of cell and developmental biology *25*, 113-132.

Graef, M., Friedman, J.R., Graham, C., Babu, M., and Nunnari, J. (2013). ER exit sites are physical and functional core autophagosome biogenesis components. Molecular biology of the cell *24*, 2918-2931.

Gueldener, U., Heinisch, J., Koehler, G.J., Voss, D., and Hegemann, J.H. (2002). A second set of loxP marker cassettes for Cre-mediated multiple gene knockouts in budding yeast. Nucleic acids research *30*, e23.

Hamasaki, M., Noda, T., and Ohsumi, Y. (2003). The early secretory pathway contributes to autophagy in yeast. Cell structure and function *28*, 49-54.

Hardwick, K.G., Boothroyd, J.C., Rudner, A.D., and Pelham, H.R. (1992). Genes that allow yeast cells to grow in the absence of the HDEL receptor. The EMBO journal *11*, 4187-4195.

Hicke, L., and Schekman, R. (1989). Yeast Sec23p acts in the cytoplasm to promote protein transport from the endoplasmic reticulum to the Golgi complex in vivo and in vitro. The EMBO journal *8*, 1677-1684.

Higashio, H., and Kohno, K. (2002). A genetic link between the unfolded protein response and vesicle formation from the endoplasmic reticulum. Biochemical and biophysical research communications *296*, 568-574.

Ishihara, N., Hamasaki, M., Yokota, S., Suzuki, K., Kamada, Y., Kihara, A., Yoshimori, T., Noda, T., and Ohsumi, Y. (2001). Autophagosome requires specific early Sec proteins for its formation and NSF/SNARE for vacuolar fusion. Molecular biology of the cell *12*, 3690-3702.

James, P., Halladay, J., and Craig, E.A. (1996). Genomic libraries and a host strain designed for highly efficient two-hybrid selection in yeast. Genetics *144*, 1425-1436.

Kakoi, S., Yorimitsu, T., and Sato, K. (2013). COPII machinery cooperates with ER-localized Hsp40 to sequester misfolded membrane proteins into ER-associated compartments. Molecular biology of the cell *24*, 633-642.

Kodera, C., Yorimitsu, T., Nakano, A., and Sato, K. (2011). Sed4p stimulates Sar1p GTP hydrolysis and promotes limited coat disassembly. Traffic *12*, 591-599.

Kung, L.F., Pagant, S., Futai, E., D'Arcangelo, J.G., Buchanan, R., Dittmar, J.C., Reid, R.J., Rothstein, R., Hamamoto, S., Snapp, E.L., *et al.* (2012). Sec24p and Sec16p

cooperate to regulate the GTP cycle of the COPII coat. The EMBO journal *31*, 1014-1027.

Kurihara, T., Hamamoto, S., Gimeno, R.E., Kaiser, C.A., Schekman, R., and Yoshihisa, T. (2000). Sec24p and Iss1p function interchangeably in transport vesicle formation from the endoplasmic reticulum in *Saccharomyces cerevisiae*. Molecular biology of the cell *11*, 983-998.

Kurokawa, K., Okamoto, M., and Nakano, A. (2014). Contact of cis-Golgi with ER exit sites executes cargo capture and delivery from the ER. Nature communications *5*, 3653.

Lee, M.C., Orci, L., Hamamoto, S., Futai, E., Ravazzola, M., and Schekman, R. (2005). Sar1p N-terminal helix initiates membrane curvature and completes the fission of a COPII vesicle. Cell *122*, 605-617.

Longtine, M.S., McKenzie, A., 3rd, Demarini, D.J., Shah, N.G., Wach, A., Brachat, A., Philippsen, P., and Pringle, J.R. (1998). Additional modules for versatile and economical PCR-based gene deletion and modification in Saccharomyces cerevisiae. Yeast *14*, 953-961.

Losev, E., Reinke, C.A., Jellen, J., Strongin, D.E., Bevis, B.J., and Glick, B.S. (2006).

Golgi maturation visualized in living yeast. Nature *441*, 1002-1006.

Malhotra, V., and Erlmann, P. (2011). Protein export at the ER: loading big collagens into COPII carriers. The EMBO journal *30*, 3475-3480.

Matsuoka, K., Orci, L., Amherdt, M., Bednarek, S.Y., Hamamoto, S., Schekman, R., and Yeung, T. (1998). COPII-coated vesicle formation reconstituted with purified coat proteins and chemically defined liposomes. Cell *93*, 263-275.

Matsuoka, K., and Schekman, R. (2000). The use of liposomes to study COPII- and COPI-coated vesicle formation and membrane protein sorting. Methods *20*, 417-428.

Matsuura-Tokita, K., Takeuchi, M., Ichihara, A., Mikuriya, K., and Nakano, A. (2006). Live imaging of yeast Golgi cisternal maturation. Nature *441*, 1007-1010.

Michelsen, K., Mrowiec, T., Duderstadt, K.E., Frey, S., Minor, D.L., Mayer, M.P., and Schwappach, B. (2006). A multimeric membrane protein reveals 14-3-3 isoform specificity in forward transport in yeast. Traffic *7*, 903-916.

Miller, E.A., Beilharz, T.H., Malkus, P.N., Lee, M.C., Hamamoto, S., Orci, L., and Schekman, R. (2003). Multiple cargo binding sites on the COPII subunit Sec24p ensure capture of diverse membrane proteins into transport vesicles. Cell *114*, 497-509.

Miller, E.A., and Schekman, R. (2013). COPII - a flexible vesicle formation system. Current opinion in cell biology *25*, 420-427.

Montegna, E.A., Bhave, M., Liu, Y., Bhattacharyya, D., and Glick, B.S. (2012). Sec12 binds to Sec16 at transitional ER sites. Plos one *7*, e31156.

Mossessova, E., Bickford, L.C., and Goldberg, J. (2003). SNARE selectivity of the COPII coat. Cell *114*, 483-495.

Nakano, A., Brada, D., and Schekman, R. (1988). A membrane glycoprotein, Sec12p, required for protein transport from the endoplasmic reticulum to the Golgi apparatus in yeast. The journal of cell biology *107*, 851-863.

Nakano, A., and Muramatsu, M. (1989). A novel GTP-binding protein, Sar1p, is involved in transport from the endoplasmic reticulum to the Golgi apparatus. The journal of cell biology *109*, 2677-2691.

Novick, P., Field, C., and Schekman, R. (1980). Identification of 23 complementation groups required for post-translational events in the yeast secretory pathway. Cell *21*, 205-215.

Okamoto, M., Kurokawa, K., Matsuura-Tokita, K., Saito, C., Hirata, R., and Nakano, A.

(2012). High-curvature domains of the ER are important for the organization of ER exit sites in *Saccharomyces cerevisiae*. Journal of cell science *125*, 3412-3420.

Orci, L., Ravazzola, M., Meda, P., Holcomb, C., Moore, H.P., Hicke, L., and Schekman, R. (1991). Mammalian Sec23p homologue is restricted to the endoplasmic reticulum transitional cytoplasm. Proceedings of the national academy of sciences of the united states of america *88*, 8611-8615.

Paccaud, J.P., Reith, W., Carpentier, J.L., Ravazzola, M., Amherdt, M., Schekman, R., and Orci, L. (1996). Cloning and functional characterization of mammalian homologues of the COPII component Sec23. Molecular biology of the cell *7*, 1535-1546.

Payne, W.E., Kaiser, C.A., Bevis, B.J., Soderholm, J., Fu, D., Sears, I.B., and Glick, B.S. (2000). Isolation of *Pichia pastoris* genes involved in ER-to-Golgi transport. Yeast *16*, 979-993.

Roberg, K.J., Crotwell, M., Espenshade, P., Gimeno, R., and Kaiser, C.A. (1999). LST1 is a SEC24 homologue used for selective export of the plasma membrane ATPase from the endoplasmic reticulum. The Journal of cell biology *145*, 659-672.

Robinson, D.G., , M.-C.H., , J.B., , R.P., &, and Ritzenthale, C. (2007). Membrane

dynamics in the early secretory pathway. Critical reviews in plant sciences *26*, 199-225.

Rossanese, O.W., Soderholm, J., Bevis, B.J., Sears, I.B., O'Connor, J., Williamson, E.K., and Glick, B.S. (1999). Golgi structure correlates with transitional endoplasmic reticulum organization in *Pichia pastoris* and *Saccharomyces cerevisiae*. The journal of cell biology *145*, 69-81.

Saito-Nakano, Y., and Nakano, A. (2000). Sed4p functions as a positive regulator of Sar1p probably through inhibition of the GTPase activation by Sec23p. Genes to cells : devoted to molecular and cellular mechanisms *5*, 1039-1048.

Saito, Y., Yamanushi, T., Oka, T., and Nakano, A. (1999). Identification of SEC12, SED4, truncated SEC16, and EKS1/HRD3 as multicopy suppressors of ts mutants of Sar1 GTPase. The journal of biochemistry *125*, 130-137.

Sato, K., and Nakano, A. (2005). Dissection of COPII subunit-cargo assembly and disassembly kinetics during Sar1p-GTP hydrolysis. Nature structural and molecular biology *12*, 167-174.

Sato, M., Sato, K., and Nakano, A. (2002). Evidence for the intimate relationship between vesicle budding from the ER and the unfolded protein response. Biochemical and

biophysical research communications *296*, 560-567.

Schwarz, K., Iolascon, A., Verissimo, F., Trede, N.S., Horsley, W., Chen, W., Paw, B.H., Hopfner, K.P., Holzmann, K., Russo, R., *et al.* (2009). Mutations affecting the secretory COPII coat component SEC23B cause congenital dyserythropoietic anemia type II. Nature genetics *41*, 936-940.

Settles, E.I., Loftus, A.F., McKeown, A.N., and Parthasarathy, R. (2010). The vesicle trafficking protein Sar1 lowers lipid membrane rigidity. Biophysical journal *99*, 1539-1545.

Shimoni, Y., Kurihara, T., Ravazzola, M., Amherdt, M., Orci, L., and Schekman, R. (2000). Lst1p and Sec24p cooperate in sorting of the plasma membrane ATPase into COPII vesicles in *Saccharomyces cerevisiae*. The journal of cell biology *151*, 973-984.

Shindiapina, P., and Barlowe, C. (2010). Requirements for transitional endoplasmic reticulum site structure and function in *Saccharomyces cerevisiae*. Molecular biology of the cell *21*, 1530-1545.

Sikorski, R.S., and Hieter, P. (1989). A system of shuttle vectors and yeast host strains designed for efficient manipulation of DNA in *Saccharomyces cerevisiae*. Genetics *122*,

19-27.

Soderholm, J., Bhattacharyya, D., Strongin, D., Markovitz, V., Connerly, P.L., Reinke, C.A., and Glick, B.S. (2004). The transitional ER localization mechanism of *Pichia pastoris* Sec12. Developmental cell *6*, 649-659.

Supek, F., Madden, D.T., Hamamoto, S., Orci, L., and Schekman, R. (2002). Sec16p potentiates the action of COPII proteins to bud transport vesicles. The journal of cell biology *158*, 1029-1038.

Tabata, K.V., Sato, K., Ide, T., Nishizaka, T., Nakano, A., and Noji, H. (2009). Visualization of cargo concentration by COPII minimal machinery in a planar lipid membrane. The EMBO journal *28*, 3279-3289.

Tan, D., Cai, Y., Wang, J., Zhang, J., Menon, S., Chou, H.T., Ferro-Novick, S., Reinisch, K.M., and Walz, T. (2013). The EM structure of the TRAPPIII complex leads to the identification of a requirement for COPII vesicles on the macroautophagy pathway. Proceedings of the National academy of sciences of the united states of america *110*, 19432-19437.

Terry, L.J., Shows, E.B., and Wente, S.R. (2007). Crossing the nuclear envelope:

hierarchical regulation of nucleocytoplasmic transport. Science *318*, 1412-1416.

Vida, T.A., Graham, T.R., and Emr, S.D. (1990). In vitro reconstitution of intercompartmental protein transport to the yeast vacuole. The journal of cell biology *111*, 2871-2884.

Watson, P., Townley, A.K., Koka, P., Palmer, K.J., and Stephens, D.J. (2006). Sec16 defines endoplasmic reticulum exit sites and is required for secretory cargo export in mammalian cells. Traffic *7*, 1678-1687.

West, M., Zurek, N., Hoenger, A., and Voeltz, G.K. (2011). A 3D analysis of yeast ER structure reveals how ER domains are organized by membrane curvature. The journal of cell biology *193*, 333-346.

Whittle, J.R., and Schwartz, T.U. (2010). Structure of the Sec13-Sec16 edge element, a template for assembly of the COPII vesicle coat. The journal of cell biology *190*, 347-361.

Yamanushi, T., Hirata, A., Oka, T., and Nakano, A. (1996). Characterization of yeast sar1 temperature-sensitive mutants, which are defective in protein transport from the endoplasmic reticulum. The journal of biochemistry *120*, 452-458.

Yang, Y.D., Elamawi, R., Bubeck, J., Pepperkok, R., Ritzenthaler, C., and Robinson, D.G. (2005). Dynamics of COPII vesicles and the Golgi apparatus in cultured *Nicotiana tabacum* BY-2 cells provides evidence for transient association of Golgi stacks with endoplasmic reticulum exit sites. Plant cell *17*, 1513-1531.

Yorimitsu, T., and Sato, K. (2012). Insights into structural and regulatory roles of Sec16 in COPII vesicle formation at ER exit sites. Molecular biology of the cell *23*, 2930-2942.

Yoshihisa, T., Barlowe, C., and Schekman, R. (1993). Requirement for a GTPase-activating protein in vesicle budding from the endoplasmic reticulum. Science *259*, 1466-1468.

Zou, S., Liu, Y., Zhang, X.Q., Chen, Y., Ye, M., Zhu, X., Yang, S., Lipatova, Z., Liang, Y., and Segev, N. (2012). Modular TRAPP complexes regulate intracellular protein trafficking through multiple Ypt/Rab GTPases in *Saccharomyces cerevisiae*. Genetics *191*, 451-460.

Publication

This research was originally published in The Journal of Biological Chemistry. Chie Kodera, et.al. Sec23 Homolog Nel1 Is a Novel GTPase-activating Protein for Sar1 but Does Not Function as a Subunit of the Coat Protein Complex II (COPII) Coat. *The Journal of Biological Chemistry*. 2014; Vol. 289: No. 31, pp. 21423–21432. © the American Society for Biochemistry and Molecular Biology.

Acknowledgments

I am grateful to my advisor, Dr. Ken Sato, Associate Professor, The University of Tokyo, for his guidance and support throughout my doctoral research. I also express my gratitude to Dr. Akihiko Nakano, Professor, The University of Tokyo, for supporting me in the early stages of my research life. He introduced me to the exciting field of vesicular transport.

I would like to thank Dr. Tomohiro Yorimitsu, Assistant Professor, Sato Laboratory, for constructive discussions. My sincere thanks go to the past and present members of Sato Laboratory and Nakano Laboratory (at The University of Tokyo and RIKEN). Dr. Takashi Ueda, Dr. Tetsuya Higashiyama, and Dr. Tomohiro Uemura provided me with valuable advice and support, and Dr. Chieko Saito has been encouraging towards all my research endeavors.

I appreciate the support of my teachers and friends at The Department of Biological Sciences, Graduate School of Science, The University of Tokyo. They have

helped me in many aspects since my years as an undergraduate student. I would like to thank the staff at The University of Tokyo and RIKEN who supported me through my graduate research.

Finally, I thank my family: my parents, my children S, K, T, and my husband Hiroyuki Miyake.

2014. 9. 16

Chie Kodera